Bayesian Focusing Transformations for Robust Coherent Adaptive Wideband Beamforming

Research Thesis

Submitted in Partial Fulfillment of the
Requirements for the Degree of
Master of Science in Electrical Engineering

Yaakov Bucris

Submitted to the Senate of the Technion - Israel Institute of Technology
Tamuz 5770 Haifa July 2010

The Research Thesis Was Done Under The Supervision of Prof. Israel Cohen from the Department of Electrical Engineering and Dr. Miriam. A. Doron from Rafael. I would like to thank both of them for their dedicated guidance, encouragement to perfection and valuable advices throughout all the stages of this research.

I would like to thank Rafael Advanced Defence Systems L.T.D for their financial and technical support on this research.

Finally, special thanks to my beloved wife, Orit and my children, Tair and Eliya-Avidan - without their love and support I could not have complete this work.

Contents

List of Figures

Abstract

Adaptive beamforming techniques are widely used in many real-world applications such as wireless communications, radar, sonar, acoustics, and seismic sensing. These techniques are effective in rejecting interference signals and noise while recovering the desired signal. In Some of the applications, wideband adaptive beamforming is requires due to the wideband nature of the employed signals.

One of the main approaches for implementing wideband adaptive beamforming is the coherent approach. Methods based on the coherent approach involve a linear pre-processor which focuses the signal subspaces at different frequencies to a single frequency, followed by a narrowband adaptive beamformer such as the Minimum Variance Distortionless Response (MVDR) algorithm. The main benefits of the coherent methods over that of non-coherent methods are low computational complexity, the ability to combat the signal cancellation problem and improved convergence capabilities.

In the literature, there are several methods to design focusing matrices for the coherent processing. The methods differ from each other in various features, such as the focused directions, optimality criteria, etc. In this thesis, we present and

study a Bayesian Focusing Transformation (BFT) for coherent wideband array processing, which is robust to uncertainties at the Direction Of Arrivals (DOAs). The Bayesian focusing approach takes into account the Probability Density Functions (PDFs) of the DOAs and minimizes the mean-square error of the transformation, thus, achieving improved focusing accuracy of the actual data over the entire bandwidth.

We also treat the important issue of robust focused MVDR beamforming in order to reduce the sensitivity of the focused MVDR beamformer to errors caused by DOAs uncertainties, Sample Matrix Inversion (SMI) implementation errors and focusing errors. We generalize the diagonal loading solution and develop a robust MVDR beamformer for the coherent wideband case referred to as the Q-loaded focused MVDR wideband beamformer. Numerical results and simulations demonstrate the superior AG of the focused Q-loaded beamformer combined with the BFT method over that of the other focusing methods.

Finally, we propose and study two robust methods for coherent focused wideband MVDR beamforming. The focusing procedure introduces a frequency dependent focusing error which causes performance degradation, especially at high Signal to Noise Ratio (SNR) values. The proposed robust methods aim at reducing the sensitivity of the coherent MVDR to focusing errors. The first method is based on modifying the beamformer optimization problem and generalizing it to bring into account the focusing transformations and the second is based on modifying the focusing scheme itself.

List of Papers

The following papers have been published or submitted for publication based on the results of some of the work described in this thesis:

1. Y. Buchris, I. Cohen and M. A. Doron, "Bayesain Focusing Transformation for Coherent Wideband Array Processing," in *Proc. 25th IEEE Convention of Electrical and Electronics Engineers in Israel, IEEEI-2008*, Eilat, Israel, pp.479-483, Dec. 2008.

2. Y. Buchris, I. Cohen and M. A. Doron, "Bayesian Focusing for Robust Adaptive Wideband Beamforming," Submitted to *IEEE Trans. Signal Processing.*

3. Y. Buchris, I. Cohen and M. A. Doron, "Robust Focusing for Wideband MVDR Beamforming," to appear in *Proc. 6th IEEE Sensor Array and Multichannel Signal Processing Workshop*, October, 2010, Israel.

Glossary

Abbreviations

AG	Array Gain
AMI	Array Manifold Interpolation
BFT	Bayesian Focusing Transformation
BI-CSSM	Beamforming-Invariance Coherent Signal Subspace Method
DF	Direction Finding
DL	Diagonal Loading
DOA	Direction Of Arrival
MUSIC	Multiple Signal Clasification
MVDR	Minimum Variance Distortionless Response
PDF	Probability Density Function
RSS	Rotational Signal Subspace
SMI	Sample Matrix Inversion
SNR	Signal to Noise Ratio
SST	Signal Subspace Transformation
UCAM	Unitary Constrained Array Manifold
WINGS	Wavefield Interpolated Narrowband Generated Subspace
WKFT	Wang-Kaveh Focusing Transformation

Alphabetic Symbols:

$\mathbf{A}_{\boldsymbol{\theta}}(w_j)$	The steering matrix in frequency w_j
$\mathbf{B}_{\tilde{\boldsymbol{\theta}}}(w_j)$	The steering matrix in frequency w_j with auxiliary DOAs
$\mathbf{b}_\theta$	Contains a basis function as its elements
$\mathbf{e}_\theta(w_j)$	The focusing error in frequency w_j
ε_j	norm of the focusing error $\mathbf{e}_\theta(w_j)$ over all possible directions
Γ	The manifold of all the possible DOAs
$\mathbf{G}(w)$	The sampling matrix
$\mathbf{g}_n(w)$	The columns of the sampling matrix $\mathbf{G}(w)$
$\mathbf{G}^\dagger(w_j)$	The pseudo-inverse of $\mathbf{G}(w_j)$.
$\{h_n(\theta)\}$	Orthogonal basis set
P	Number of sources
K	Number of snapshots
J	Number of frequency bins
N	The number of sensors in the array
k	The wave number
T_s	The sampling frequency
$\mathbf{r}_m$	the coordinates of the mth sensor
$\mathbf{T}(w_j)$	The focusing matrix in frequency w_j
$\mathbf{T}_{WKFT}(w_j)$	WKFT focusing matrix
$\mathbf{T}_{RSS}(w_j)$	RSS focusing matrix
$\mathbf{T}_{WINGS}(w_j)$	RSS focusing matrix
$\mathbf{T}_{BFT}(w_j)$	RSS focusing matrix
$\mathbf{X}(w_j)$	Frequency domain received data vector at frequency w_j
$\mathbf{x}(w)$	Output of any array of arbitrary geometry

$\mathbf{x}_k(w_j)$	The kth snapshot frequency domain vector of the input signal
$\mathbf{s}_k(w_j)$	The frequency domain vector of the sources
$\mathbf{n}_k(w_j)$	The frequency domain vector of the additive noise
$y(w_j)$	Output of the narrowband beamformer at frequency w_j
$y_{Non\_Coherent}(n)$	The temporal beamformer output vector
$\boldsymbol{\theta}$	The DOAs vector
$\tilde{\boldsymbol{\theta}}$	Vector of auxiliary DOAs
$\mathbf{U}(w_j)$	Contains the left singular vectors of $\mathbf{A}_{\boldsymbol{\theta}}(w_j)\mathbf{A}_{\boldsymbol{\theta}}(w_0)^H$
$\mathbf{V}(w_j)$	Contains the right singular vectors of $\mathbf{A}_{\boldsymbol{\theta}}(w_j)\mathbf{A}_{\boldsymbol{\theta}}(w_0)^H$
$\mathbf{w}_\theta(w)$	Coefficient vector of a beamformer in frequency w
$\hat{\mathbf{w}}_\theta^f$	Coefficient vector of the focused beamformer
$\mathbf{y}_k(n)$	The temporal focused vector
$\mathbf{R}_\mathbf{x}(w)$	Covariance matrix in frequency w
$\hat{\mathbf{R}}_\mathbf{x}(w)$	maximum likelihood estimate of $\mathbf{R}_\mathbf{x}(w)$
$\hat{\mathbf{R}}_\mathbf{x}^f$	The covariance matrix of the focused vector $\mathbf{y}_k(n)$
$\mathbf{a}_\theta(w)$	Steering vector in frequency w and the direction θ
$\tilde{\mathbf{n}}_k(n)$	The focused noise vector
T_0	Design parameter of the diagonal loading
β	Loading coefficient
λ_i	Eigenvalues of the covariance matrix

Φ_i	Eigenvectors of the covariance matrix
$\mathbf{U}_N$	The noise subspace
$f(\theta)$	The minimization function of the MUSIC algorithm
$x_n(t)$	The nth sensor output
τ_{np}	The delays associated with the signal propagation time
$\{s_p(t)\}_{p=1}^{P}$	The radiated wideband signals processes
$\{n_n(t)\}_{n=1}^{N}$	The additive noise processes
$\sigma_n^2(w_j)\mathbf{I}$	The covariance matrix of the noise
$\mathbf{R}_s(w_j)$	The covariance matrix of the sources
$\{\theta_i\}_{i=1}^{P}$	The DOAs - modelled as random variables
$f_{\theta_i}(\theta)$	Probability Density Functions (PDFs) of the DOAs
$\rho(\theta)$	The weighting function of the BFT
$\mathbf{C}(w)$	the orthogonal decomposition of the product $\rho(\theta)\mathbf{a}_\theta(w)$
f_0	The focusing frequency
f_c	The carrier frequency
d	Spacing between two adjacent sensors
$\hat{\theta}_{i\_DF}$	The estimate of the DF algorithm
$\sigma_{n_{out}}^2$	The output noise power of the focused beamformer
$\mathbf{Q}$	The Q-loading matrix
$\mathbf{w}_\theta^{f,QL}$	The coefficient vector of the Q-loaded beamformer
$\Delta g_m(w_j)$	A zero-mean complex gain error of the mth sensor
$\sigma_g^2(w_j)$	The variance of $\Delta g_m(w_j)$
ξ	The input SNR
$\mathcal{P}\{\cdot\}$	denotes the *principal eigenvector* of a matrix

Chapter 1

Introduction

1.1 Motivation and Goals

Adaptive beamforming techniques are used for sensors arrays to enhance the signal-to-interference plus noise ratio in many applications such as wireless communications, radar, sonar, acoustics, and seismic sensing. These techniques are effective in rejecting interference signals whose incident directions of arrival differ from that of the desired signal [1]. The potential of adaptive beamforming was already recognized since the early 1960's for the narrowband case. Yet, in the last two decades, the necessity for wideband adaptive beamforming increased with the development of third and fourth generations of wireless communications for mobile systems as well as ultra-wideband communication systems [2–5]. These systems support very high data rate communications due to their wideband nature combined with their space-time processing abilities.

Wideband adaptive beamforming techniques can be classified into two main

categories. The first category consists of non-coherent wideband beamforming methods which employ either time domain or frequency domain implementations. The non-coherent time domain techniques utilize multi-tap spatial adaptive filters whose coefficients are adjusted to suppress the interferences while preserving the desired signal (e.g. [2], [6]). The non-coherent frequency domain techniques implement a narrowband adaptive beamformer in each frequency bin [1]. All the methods associated with the non-coherent category are computationally expensive, have a slow convergence rate due to a large number of adaptive coefficients, and are prone to signal cancellation problem in coherent multi-source scenarios.

The second category consists of coherent methods for wideband adaptive beamforming which incorporate a focusing procedure for signal subspace alignment, originally proposed by Wang and Kaveh [7] for Direction of Arrivals (DOAs) estimation applications. The focusing procedure involves a pre-processor implemented as a linear transformation matrix which focuses the signal subspaces at different frequencies to a single frequency, followed by a narrowband adaptive beamformer such as the Minimum Variance Distortionless Response (MVDR) algorithm (see Sec. 1.2.4) or a DOAs estimator such as the Multiple Signal Classification (MUSIC) algorithm (see Sec. 1.2.6). The main benefits of the coherent methods are low computational complexity, the ability to combat the signal cancellation problem and improved convergence properties. Although the preliminary works on coherent array processing were aimed at DOAs estimation applications [7–9], following works on coherent processing for wideband adaptive beamforming appeared in the early 90's [10–14].

In the literature, there are two basic approaches to design focusing matrices. The first approach utilizes schemes requiring a-priori knowledge of the DOAs of the sources using them as focusing directions, e.g. [7, 8]. In [9], a unitary focusing transformation named as the Rotational Signal Subspace(RSS), is designed and analyzed to provide focused data at a preliminary estimated DOAs. The advantage of the unitary focusing transformation is that there is no focusing loss which is a measure to the degradation in the Signal to Noise (SNR) due to the focusing operation. This RSS focusing method was extended by Doron and Weiss in [15] where a general class of focusing matrices were proposed, referred to as Signal Subspace Transformation (SST) focusing matrices, designed to generate sufficient statistics for maximum likelihood bearing estimation. The contribution of Hang and Mao [16] is to design a class of robust focusing matrices called Unitary Constrained Array Manifold (UCAM) focusing, which reduces the sensitivity of the RSS to variations of DOA estimates by focusing in all the DOAs lying around a vicinity of the actual DOAs. All the above cited works, share the same characteristic of requiring initial DOAs estimates, which introduce additional computational burden and sensitivity to DOAs uncertainties, and will be referred to as the directional focusing approach.

The second approach consists of spatial interpolation methods which focus all angular directions. Doron et.al [17] propose the Array Manifold Interpolation (AMI) which does not require DOA estimates, yet, requires the array to satisfy the spatial sampling condition. Other similar works that employ spatial resampling can be found at [12, 18–21]. In [22] an interpolation based focusing

approach called Wavefield Interpolated Narrowband Subspace (WINGS) method is proposed which is developed using the wavefield modelling theory [23]. It provides a closed form expression to the transformation and to its focusing error. Based on the WINGS, two robust extensions are developed aiming at controlling the noise gain of the transformation. A DOA independent focusing method based upon the idea of frequency-invariant beamspace processing was proposed in [19], and referred to as Beamforming-Invariance Coherent Signal Subspace Method (BI-CSSM). Kashavarz [20] propose a focusing method which does not require DOA estimates is applied together with a frequency dependent weighting function which is proportional to the power spectral density of the pulse. We refer to the interpolation based approach as the *panoramic* focusing approach. The directional approach achieves relatively small focusing errors but is sensitive to DOAs uncertainties, while the panoramic approach does not require any knowledge of the DOAs, however it typically has higher error levels, since it attempts to focus all directions.

There are also focusing methods which provide a compromise between the directional and panoramic approaches by perform the focusing in angular sectors. A numerical method for focusing within an angular sector is proposed and studied at [21]. Sellone [24] derive a unitary focusing approach which incorporates a deterministic weighting function. A numerical solution to the optimization problem is derived and studied in the paper.

In addition to the presented studies dealing with the design of focusing transformations with desired properties such as unitary, there are papers on employing the

existing focusing methods in order to improve and develop DF and beamforming algorithms. Feng et.al [25] develop a new high resolution DF algorithm for wideband signals and test its performance with various focusing methods. Both [26] and [27] present a robust DF algorithm for the coherent wideband case which take into account array calibration errors and mutual coupling effects. Claudio [28, 29] present and study a steered wideband adaptive beamformer, optimized by Maximum Likelihood criterion in the light of a general reverberation model. It employs a focusing transformation which focuses only in the desired source direction, thus yielding a diagonal focusing transformation.

Most of the focusing methods in the academic literature belong to either the directional approach requiring a-priori knowledge of the DOAs or the panoramic approach where no a-priori knowledge is required. Methods which focus in sectors employ a deterministic weighting function and provide a numerical solution. Our first goal in to design a focusing procedure which is a compromise between the directional focusing approach and the panoramic focusing approach by incorporating statistical information about the DOAs, thus, enjoying the benefits of both approaches. To this end, we use a Bayesian formalism in which we take into account the uncertainty of the DOAs by modelling them as random variables with a given prior statistics. We derive a closed-form solution to a Bayesian Focusing Transformation (BFT) minimizing the Mean-Square Error (MSE) of the transformation, thus achieving improved focusing accuracy over the entire bandwidth.

The output of the focusing procedure is a vector with a narrowband array response, thus, any narrowband adaptive beamforming algorithm may be applied,

such as the well-known Capon beamformer [30] ,also referred to as the Minimum Variance Distortionless Response (MVDR) beamformer. The theoretic performance of the MVDR beamformer is better than that of the conventional beamformer. Yet, it has a substantial performance degradation due to array calibration errors, DOAs errors [4], and the SMI estimation errors [5]. In the focused MVDR beamformer, the focusing error also comes into play and may deteriorate the performance. One of the common methods to reduce the sensitivity of the MVDR beamformer to array calibration errors is via diagonal loading of the sample covariance matrix [31]. Diagonal loading was originally proposed for the narrowband case, and it was shown to effectively reduce the sensitivity of the MVDR. Our second goal is to derive an extension of the diagonal loading solution for the coherent wideband case, in order to increase the robustness against mismatch and focusing errors, and improve the performance of the MVDR.

We tested the performance of the Bayesian approach combined with the robust MVDR loading algorithm and compared to other focusing methods (to be discussed at Sec 1.2). One of the prominent problems we saw in the simulation is the sensitivity of the focused MVDR beamformer at high SNR values. Our third goal is to investigate this sensitivity and show analytically that it is caused by the focusing errors at the desired source direction. In order to reduce the sensitivity of the coherent MVDR beamformer to focusing errors at the desired source direction, we propose and study two robust methods for coherent focused wideband MVDR beamforming. The first method modifies the MVDR algorithm to take into account the various errors and the second is based on modifying the focusing transformation

so that the focusing error is reduced in the direction of the desired source.

1.2 Background

Coherent wideband adaptive beamforming techniques, based on the signal subspace alignment [7, 9] concept, achieve an improved performance over that of the non-coherent wideband adaptive beamformer [1, 2]. The non-coherent wideband adaptive beamformer is implemented in the frequency domain as a narrowband beamformer for each frequency bin. Fig.1.1 shows a general block diagram for the non-coherent wideband adaptive beamformer. For each frequency bin, a narrowband adaptive beamformer is applied to the frequency domain data vector $\mathbf{X}(f_j)= [x_1(f_j), .., x_N(f_j)]^H$, $j = 1, .., J$. The outputs of all the narrowband beamformers, $y(f_j)$, $j = 1, .., J$, are collected and fed into an inverse FFT block yielding the temporal beamformer output vector, $y_{Non\_Coherent}(n)$. The non-coherent beamformer is computationally expensive, has a slow convergence rate due to a large number of adaptive coefficients and is prone to signal cancellation problem in coherent source scenarios.

Fig.1.2 presents a general block diagram for the focused wideband adaptive beamformer. This approach involves a pre-processor implemented as a frequency dependent linear transformation matrix $\mathbf{T}(w_j)$ which focuses the signal subspaces at different frequencies to a single frequency, followed by a single time domain narrowband beamformer. The main benefits of the coherent approach are low computational complexity, the ability to combat signal cancellation problem and

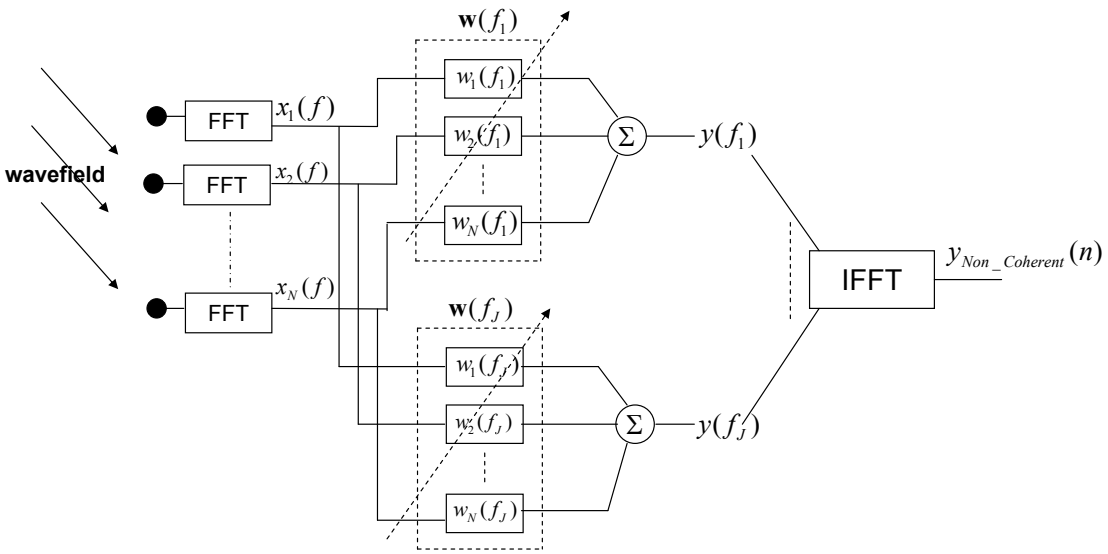

Figure 1.1: Block diagram of the non-coherent wideband adaptive beamformer.

improved convergence properties. The focusing transformation, $\mathbf{T}(w_j)$ should satisfy the following

$$\mathbf{T}(w_j)\mathbf{A}_{\boldsymbol{\theta}}(w_j) \cong \mathbf{A}_{\boldsymbol{\theta}}(w_0), \tag{1.1}$$

where w_j are the frequencies within the bandwidth of the signals and w_0 is the focused frequency, i.e. $\mathbf{T}(w_j)$ focuses the signal subspaces $\mathbf{A}_{\boldsymbol{\theta}}(w_j)$ at frequencies $\{w_j\}$ onto the signal subspace $\mathbf{A}_{\boldsymbol{\theta}}(w_0)$. The matrices $\mathbf{A}_{\boldsymbol{\theta}}(w_j)$ and $\mathbf{A}_{\boldsymbol{\theta}}(w_0)$ contain the steering vectors of the sources in their columns at frequencies w_j and w_0, respectively, where $\boldsymbol{\theta}$ is the DOAs vector.

There are several approaches to design the focusing matrix $\mathbf{T}(w_j)$ (see Sec.1.1). In the following sections, we describe several representative focusing methods. We use them during this work in order to compare their performance with that of the

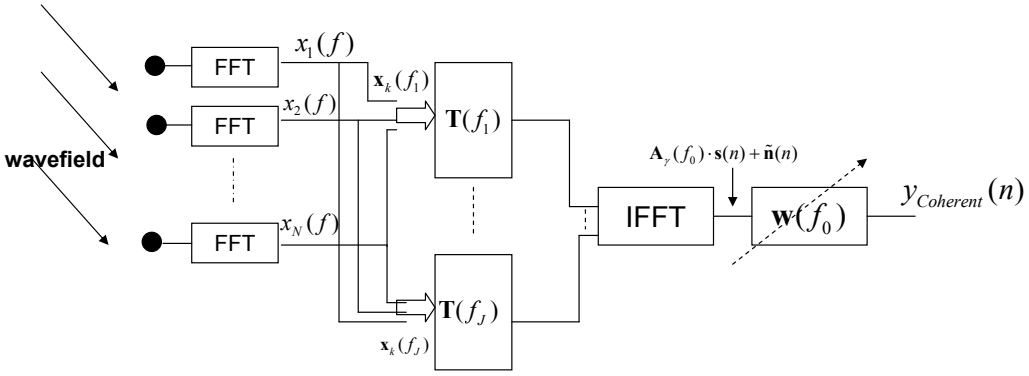

Figure 1.2: Block diagram of the coherent wideband adaptive beamformer.

innovative Bayesian focusing transformation which is proposed in Chapter 2.

1.2.1 Wang-Kaveh Focusing Transformation (WKFT)

In the pioneering work of [7], a focusing transformation which require a-priori knowledge of the sources' DOAs vector is derived. We name this focusing method as Wang and Kaveh Focusing transformation (WKFT). WKFT attempts to find a set of matrices $\mathbf{T}(w_j), j = 1, ..J$ which satisfy the following

$$\mathbf{T}(w_j)\mathbf{A}_{\boldsymbol{\theta}}(w_j) \cong \mathbf{A}_{\boldsymbol{\theta}}(w_0), j = 1, 2, .., J, \tag{1.2}$$

Where $\mathbf{A}_{\boldsymbol{\theta}}(w_j)$ is a matrix constructed from the steering vectors at the directions specified by the vector $\boldsymbol{\theta}$. The desired transformation $\mathbf{T}(w_j)$ is given by

$$\mathbf{T}_{WKFT}(w_j) = [\mathbf{A}_{\boldsymbol{\theta}}(w_0)|\mathbf{B}_{\tilde{\boldsymbol{\theta}}}(w_0)]\,[\mathbf{A}_{\boldsymbol{\theta}}(w_j)|\mathbf{B}_{\tilde{\boldsymbol{\theta}}}(w_j)]^{\dagger} \tag{1.3}$$

where † denotes the pseudo-inverse of $[\mathbf{A}_{\boldsymbol{\theta}}(w_j)|\mathbf{B}_{\tilde{\boldsymbol{\theta}}}(w_j)]$. $\mathbf{B}_{\tilde{\boldsymbol{\theta}}}(w_j)$ and $\mathbf{B}_{\tilde{\boldsymbol{\theta}}}(w_0)$ are the direction matrices at frequencies w_j and w_0, respectively, with auxiliary angles specified by the vector $\tilde{\boldsymbol{\theta}}$, aimed at reducing the high sensitivity to inaccurate knowledge of the DOAs vector $\boldsymbol{\theta}$. WKFT achieves relatively low focusing errors and superior performance when the DOAs vector is known perfectly, yet, it has a high sensitivity to DOAs uncertainties. This sensitivity is somewhat reduced due to the addtion of the auxiliary angles specified by the vector $\tilde{\boldsymbol{\theta}}$.

1.2.2 Rotational Signal Subspace Focusing Transformation(RSS)

In [9] a quantitive measure for the focusing loss is defined as the ratio of array SNR after and before focusing operation. The authors point out the merit of using unitary focusing matrices since they have no focusing loss. They propose unitary transformations satisfying the following constraint minimization problem

$$\min_{\mathbf{T}(w_j)} \left\|\mathbf{A}_{\boldsymbol{\theta}}(w_0) - \mathbf{T}(w_j)\mathbf{A}_{\boldsymbol{\theta}}(w_j)\right\|_F, j = 1, 2, ..J \tag{1.4}$$

subject to

$$\mathbf{T}^H(w_j)\mathbf{T}(w_j) = \mathbf{I}, \tag{1.5}$$

where $\|\cdot\|_F$ is the Frobenious matrix norm [32]. The solution to (1.4) is given by

$$\mathbf{T_{RSS}}(w_j) = \mathbf{V}(w_j)\mathbf{U}(w_j)^H \tag{1.6}$$

where the columns of $\mathbf{U}(w_j)$ and $\mathbf{V}(w_j)$ are the left and right singular vectors of $\mathbf{A}_{\boldsymbol{\theta}}(w_j)\mathbf{A}_{\boldsymbol{\theta}}(w_0)^H$. They named this focusing matrix the Rotational Signal Subspace (RSS) focusing matrix. Similarly to the WKFT, adding auxiliary angles is recommended in order to reduce sensitivity to inaccurate knowledge of the DOAs vector.

1.2.3 Wavefield Interpolated Narrowband Generated Subspace Focusing Transformation(WINGS)

Both WKFT and RSS focusing methods require preliminary estimates of the DOA vector. In the literature, there exist several focusing methods based on spatial interpolation (e.g. [12, 17–21]). These focusing methods have the advantage of being data independent but at cost of higher focusing errors than those of the directional focusing methods. One of these method, proposed Recently by Doron et al. [22], is the Wavefield Interpolated Narrowband Generated Subspace (WINGS) focusing method.

The WINGS focusing method [22] is based on the wavefield modelling formalism [23] according to which, the output of almost any array $\mathbf{x}(w)$ of arbitrary geometry can be written as a product of array geometry dependent part and wavefield dependent part, i.e. $\mathbf{x}(w) = \mathbf{G}(w)\psi(w)$ where $\mathbf{G}(w)$ is a sampling matrix which is independent of the wavefield and the coefficient vector $\psi(w)$ is independent of the array. Using the wavefield modelling formalism, the steering vector can be

expressed by terms of orthogonal decomposition

$$\mathbf{a}_\theta(w) = \sum_n \mathbf{g}_n(w) h_n^*(\theta), \tag{1.7}$$

where $\mathbf{g}_n(w)$ are the columns of the sampling matrix $\mathbf{G}(w)$ and $\{h_n(\theta)\}$ is an orthogonal basis set in $\mathbf{L}_2(\Gamma)$, where Γ is the manifold of all the possible DOAs. In 2-D, we use the Fourier basis, i.e. $h_n(\theta) = \frac{1}{\sqrt{2\pi}} e^{-in\theta}$. The WINGS focusing transformation $\mathbf{T}(w_j)$ minimizes ε_j, the L_2 norm of the focusing error $\mathbf{e}_\theta(w_j)$ over all possible directions

$$\varepsilon_j^2 \triangleq \frac{1}{N} \int_{\theta\,=\,-\pi}^{\pi} d\theta \left\| \mathbf{e}_\theta(w_j) \right\|^2 . \tag{1.8}$$

where

$$\mathbf{e}_\theta(w_j) = \mathbf{a}_\theta(w_0) - \mathbf{T}(w_j)\mathbf{a}_\theta(w_j) \quad \forall\theta. \tag{1.9}$$

Using (1.7), the focusing error can be expressed as

$$\mathbf{e}_\theta(w_j) = \left[\mathbf{G}(w_0) - \mathbf{T}(w_j)\mathbf{G}(w_j)\right] \mathbf{b}_\theta, \tag{1.10}$$

where the vector $\mathbf{b}_\theta$ contains the basis functions $\{h_n(\theta)\}$ as its elements. Thus, one may consider (1.10) to be the orthogonal decomposition of the error vector $\mathbf{e}_\theta(w_j)$. We can apply Paraseval's identity on 1.8 and derive the following Least-Square(LS) minimization problem

$$\varepsilon_j^2 = \frac{1}{N} \left\| \mathbf{G}(w_0) - \mathbf{T}(w_j)\mathbf{G}(w_j) \right\|_F^2 . \tag{1.11}$$

The WINGS focusing matrix minimizing (1.11) is given by

$$\mathbf{T}(w_j) = \mathbf{G}(w_0)\mathbf{G}^{\dagger}(w_j), \tag{1.12}$$

where $\mathbf{G}^{\dagger}(w_j)$ denotes the pseudo-inverse of $\mathbf{G}(w_j)$.

1.2.4 The Minimum Variance Distortionless Response (MVDR) beamformer

After the focusing procedure, one may applied any narrowband adaptive beamforming algorithm such as the well-known MVDR beamformer [30]. The MVDR algorithm minimizes the array output power subject to a distortionless constraint on the desired source direction. The narrowband MVDR weight vector is the solution to the following minimization problem

$$\min_{\mathbf{w}_\theta(w)} \mathbf{w}_\theta(w)^H \mathbf{R}_{\mathbf{x}}(w)\mathbf{w}_\theta(w), \tag{1.13a}$$

subject to the distortionless constraint,

$$\mathbf{w}_\theta^H(w)\mathbf{a}_\theta(w) = 1, \tag{1.13b}$$

where $\mathbf{R}_{\mathbf{x}}(w)$ is the covariance matrix of the narrowband received vector $\mathbf{x}(w)$ at frequency w and $\mathbf{a}_\theta(w)$ is the steering vector in frequency w and the direction θ.

The solution to the above minimization problem is (see e.g. [1])

$$\mathbf{w}_\theta(w) = \frac{\mathbf{R}_\mathbf{x}^{-1}(w)\mathbf{a}_\theta(w)}{\mathbf{a}_\theta^H(w)\mathbf{R}_\mathbf{x}^{-1}(w)\mathbf{a}_\theta(w)}. \tag{1.14}$$

In (1.14) the inversion of the covariance matrix $\mathbf{R}_\mathbf{x}(w)$ is required. Since $\mathbf{R}_\mathbf{x}(w)$ is unknown one may use the maximum likelihood estimate of $\mathbf{R}_\mathbf{x}(w)$ from snapshots of the data samples

$$\hat{\mathbf{R}}_\mathbf{x}(w) = \frac{1}{K}\sum_{k=1}^{K}\mathbf{x}_k(w)\mathbf{x}_k^H(w). \tag{1.15}$$

This method is known as the Sample Matrix Inversion (SMI) method.

The MVDR algorithm was originally proposed for the narrowband case, yet, it can be extended to the wideband case. In the literature there are two methods to perform wideband array processing using the MVDR algorithm. The first method employs a non-coherent processing as depicted at Fig. 1.1. The second method is the coherent processing employs a focusing transformations as depicted at Fig. 1.2. Let us first review the non-coherent wideband MVDR beamformer and then describe the focused wideband MVDR beamformer.

Non-coherent MVDR-SMI adaptive beamformer

The non-coherent wideband MVDR - SMI method is implemented in the frequency domain by applying a narrowband beamformer at each frequency bin (see e.g. [1]). A DFT is first performed followed by the estimation of the narrowband sample

covariance matrix at each frequency bin

$$\hat{\mathbf{R}}_{\mathbf{x}}(w_j) = \frac{1}{K}\sum_{k=1}^{K}\mathbf{x}_k(w_j)\mathbf{x}_k^H(w_j). \tag{1.16}$$

The narrowband MVDR - SMI adaptive weight vector is then computed at each frequency bin as

$$\hat{\mathbf{w}}_\theta(w_j) = \frac{\hat{\mathbf{R}}_{\mathbf{x}}^{-1}(w_j)\mathbf{a}_\theta(w_j)}{\mathbf{a}_\theta^H(w_j)\hat{\mathbf{R}}_{\mathbf{x}}^{-1}(w_j)\mathbf{a}_\theta(w_j)}. \tag{1.17}$$

The adaptive weights (1.17) may now be used to perform the actual beamforming at each frequency bin yielding the non-coherent adaptive beamformer output, in the frequency domain.

Coherent MVDR-SMI focused adaptive beamformer

The MVDR-SMI focused adaptive beamformer may be simply implemented as a narrowband adaptive beamformer operating on the temporal focused data vector $\mathbf{y}_k(n)$ where $\mathbf{y}_k(n) = \sum_{l=1}^{J}\mathbf{T}(w_l)\mathbf{x}_k(w_l)e^{jw_l nT_s} = \mathbf{A}_{\boldsymbol{\theta}}(w_0)\mathbf{s}_k(n) + \tilde{\mathbf{n}}_k(n)$ (see Fig.1.2) whose sample covariance matrix is estimated by

$$\hat{\mathbf{R}}_{\mathbf{x}}^f = \frac{1}{KJ}\sum_{k,n}\mathbf{y}_k(n)\mathbf{y}_k^H(n). \tag{1.18}$$

The focused coherent adaptive beamformer MVDR weight vector is simply computed in the time domain by

$$\hat{\mathbf{w}}_\theta^f = \frac{\left(\hat{\mathbf{R}}_{\mathbf{x}}^f\right)^{-1}\mathbf{a}_\theta(w_0)}{\mathbf{a}_\theta^H(w_0)\left(\hat{\mathbf{R}}_{\mathbf{x}}^f\right)^{-1}\mathbf{a}_\theta(w_0)}, \tag{1.19}$$

where w_0 is the focusing frequency and f stands for *focused* beamformer.

1.2.5 Robust MVDR Beamforming

The MVDR beamformer is known to have superior resolution and interference rejection capabilities, provided that the array steering vector corresponding to the DOA of the desired signal is accurately known. In practice, it is often the case, due to array calibration errors and inaccurate knowledge of the source direction, that the performance of the MVDR beamformer may deteriorate below that of the conventional beamformer [31]. Furthermore, the MVDR-SMI implementation is sensitive to estimation errors in the sample covariance matrix [33]. In the coherent wideband case, the focused MVDR beamformer will exhibit an additional sensitivity to the focusing errors. Many robust schemes constraint the Euclidian norm of the beamformer coefficient vector, thus decreasing the sensitivity to various modelling errors.

Diagonal loading has been a popular approach to improve the robustness of the MVDR beamformer [1, 33–35]. It is derived by imposing an additional quadratic constraint either on the Euclidian norm of the weight vector itself or on its difference from the nominal weight vector. In its common formalism, the diagonal loading solves the following minimization problem

$$\min_{\mathbf{w}_\theta(w)} \mathbf{w}_\theta^H(w)\mathbf{R}_\mathbf{x}(w)\mathbf{w}_\theta(w), \tag{1.20a}$$

subject to the distortionless constraint,

$$\mathbf{w}_\theta(w)^H \mathbf{a}_\theta(w) = 1, \tag{1.20b}$$

and the quadratic constraint,

$$\mathbf{w}_\theta(w)^H \mathbf{w}_\theta(w) \leq T_0. \tag{1.20c}$$

It can be shown that the solution to (1.24) is given by [1]

$$\mathbf{w}_\theta(w) = \frac{\left(\mathbf{R}_\mathbf{x}(w) + \beta\mathbf{I}\right)^{-1} \mathbf{a}_\theta(w)}{\mathbf{a}_\theta^H(w) \left(\mathbf{R}_\mathbf{x}(w) + \beta\mathbf{I}\right)^{-1} \mathbf{a}_\theta(w)}, \tag{1.21}$$

where β is the Lagrange multiplier which is determined in such a way that the quadratic constraint is satisfied.

Later, we generalize the diagonal loading solution to the focused wideband MVDR beamformer.

1.2.6 The Multiple Signal Classification (MUSIC) Algorithm

Focusing methods belonging to the directional approach such as WKFT and RSS, require preliminary estimate of the DOAs vector. One of the widespread DOAs estimation algorithm is the Multiple Signal Classification (MUSIC) algorithm, Originally proposed by [36], which is a subspace based algorithm. The basic principle of this algorithm is to use the orthogonality between the signal subspace and the

noise subspace. The MUSIC algorithm was originally proposed for the narrowband case, yet, it can be extended easily for the wideband case.

The input of the narrowband MUSIC algorithm is the narrowband covariance matrix or an estimated version of it (1.16). The covariance matrix can be written by terms of its eigenvalues and eigenvectors as

$$\hat{\mathbf{R}}_{\mathbf{x}}(w_j) = \sum_{i=1}^{N} \lambda_i \Phi_i \Phi_i^H \tag{1.22}$$

The P eigenvectors which correspond to the P largest eigenvalues spread the signal subspace which is identical to the space spread by the steering vectors. The remaining eigenvectors are the noise subspace. We define the noise subspace as

$$\mathbf{U}_N = \left[\Phi_{P+1} \vdots \Phi_{P+1} \vdots \cdots \vdots \Phi_N \right] \tag{1.23}$$

The signal subspace and and the noise subspace are orthogonal subspaces. Thus, the following is satisfied:

$$\left\| \mathbf{a}_{\theta_i}(w_j) \mathbf{U}_N \right\|^2 = 0, \quad i = 1, 2, ..P \tag{1.24}$$

The MUSIC algorithm define the function $f(\theta) = \left\| \mathbf{a}_{\theta}(w_j) \mathbf{U}_N \right\|^2$ and choose the P minima of $f(\theta)$ or equivalently the P maxima of $\frac{1}{f(\theta)}$ over $-\pi \leq \theta \leq \pi$. For the coherent wideband case we find the noise subspace $\mathbf{U}_N$, spread by the eigenvectors of the focused covariance matrix (1.18).

1.3 Organization

In Chapter 2, we formulate the problem of interest and define the optimal MMSE BFT problem which is designed to handle DOA uncertainties. We derive a closed form expression for the BFT as a weighted extension to the WINGS method. We demonstrate the focusing error of the BFT and compare it to that of other focusing methods. A time progressing algorithm is suggested which incorporates a direction findings stage followed by the focused beamformer.

In Chapter 3 we derive the robust focused Q-loaded MVDR beamformer and analyze its performance. A performance analysis of the robust Bayesian focused MVDR beamformer is conducted and compared to that of focusing methods.

In Chapter 4 a numerical and simulative study for the single source case is conducted using the WINGS focusing method. We choose to consider WINGS as a test case since it is a panoramic focusing methods which introduces relatively high focusing errors. We derive an analytic approximation to the degradation of the AG and show analytically that this degradation occurs due to focusing error in the desired source direction. In order to reduce this performance degradation, two robust schemes are proposed.

We Conclude in Chapter 5 with a summary and discussion on future research directions.

Chapter 2

Bayesian Focusing Transformations

2.1 Introduction

Wideband coherent adaptive beamforming techniques incorporate a focusing procedure for signal subspace alignment [7, 9, 11]. The focusing procedure involves a pre-processor implemented as a linear transformation matrix which focuses the signal subspaces at different frequencies to a single frequency, followed by a narrowband beamformer. There are two basic approaches to design focusing matrices. The first approach utilizes schemes requiring a-priori knowledge of the sources' DOAs using them as focusing directions e.g. [7, 9], and will be referred to as the directional focusing approach. The second approach consists of spatial interpolation methods which focus all angular directions [12, 18, 22] and will be referred to as the panoramic focusing approach . The first approach achieves relatively small

focusing errors but is sensitive to DOA uncertainties, while the later approach does not require any knowledge of the DOAs, however it typically has higher error levels, since it attempts to focus all directions. Furthermore, the spatial interpolation process requires that the array satisfy the spatial sampling condition [23].

In this chapter, we propose a third approach, namely the Bayesian approach for focusing transformation design. In the Bayesian approach we take into account the uncertainty of the DOAs by modelling them as random variables with a given prior statistics. We derive a Bayesian Focusing Transformation (BFT) minimizing the Mean-Square Error (MSE) of the transformation, thus achieving improved focusing accuracy over the entire bandwidth. The proposed Bayesian focusing transformation is a compromise between the directional focusing approach, which requires preliminary DOA estimates, and the spatial interpolation based panoramic focusing approach, which does not require any apriori DOA knowledge. In fact, BFT can be view as a generalization which includes the two approaches as special cases. The close-form solution to the Bayesian focusing problem is based on an extension of the WINGS focusing method.

This chapter is organized as follows: In Section 2.2 we formulate the problem of interest. In Section 2.3 we define the optimal MMSE BFT problem which is designed to handle DOA uncertainties. Next, in Section 2.4 we develop a weighted extension to the WINGS method which is then used to get a closed form expression for the BFT. In section 2.5 we present a simulation example for the case of DOA uncertainties and compare the focusing error of the BFT to that of other focusing methods discussed in the previous chapter. In Section 2.6, a time progressing

algorithm is proposed which incorporates a Direction Finding (DF) stage operating on the focused data followed by the Bayesian focused beamformer. Finally we summarize this chapter in section 2.7.

2.2 Problem Formulation

Consider an arbitrary array of N sensors sampling a wavefield generated by P statistically independent wideband sources, in the presence of additive noise. For simplicity, we confine our discussion to the free and far field model. The signal measured at the output of the nth sensor can be written as

$$x_n(t) = \sum_{p=1}^{P} s_p(t - \tau_{np}) + n_n(t), \;\; n = 1, .., N, \tag{2.1}$$

where $\{s_p(t)\}_{p=1}^{P}$ and $\{n_n(t)\}_{n=1}^{N}$ denote the radiated wideband signals and the additive noise processes, respectively. The parameters $\{\tau_{np}\}$ are the delays associated with the signal propagation time from the pth source to the nth sensor. Let $\{\gamma_i\}_{i=1}^{P}$ be the DOAs of the sources, $\gamma \equiv \theta$ in 2-D and $\gamma \equiv (\theta, \varphi)$ in 3-D where θ is the azimuth angle and φ is the elevation angle. For simplicity, we restrict ourselves to the 2-D case. Each T seconds of received data are divided into K snapshots and transformed to the frequency domain yielding in matrix formalism the following expression

$$\mathbf{x}_k(w_j) = \mathbf{A}_{\boldsymbol{\theta}}(w_j)\mathbf{s}_k(w_j) + \mathbf{n}_k(w_j), \qquad j = 1, 2, ...J, \;\; k = 1, 2, ...K, \tag{2.2}$$

where $\mathbf{x}_k(w_j)$, $\mathbf{s}_k(w_j)$ and $\mathbf{n}_k(w_j)$ denote vectors whose elements are the discrete Fourier coefficients of the measurements, of the unknown sources signals and of the noise, respectively at the kth snapshot and frequency w_j, J is the number of frequency bins, and $\mathbf{A}_{\boldsymbol{\theta}}(w_j)$ is the $N \times P$ direction matrix

$$\mathbf{A}_{\boldsymbol{\theta}}(w_j) \equiv [\mathbf{a}_{\theta_1}(w_j), \mathbf{a}_{\theta_2}(w_j), ..., \mathbf{a}_{\theta_P}(w_j)]. \tag{2.3}$$

The vector $\mathbf{a}_\theta(w)$, referred to as the *array manifold* vector, is the response of the array to an incident plane wave at frequency w and DOA θ. For an array comprised of identical omni-directional uncoupled sensors in free field, the *array manifold* vector is

$$[\mathbf{a}_\theta(w)]_m = \exp\left\{ik\mathbf{r}_m \cdot \hat{\boldsymbol{\theta}}\right\}, \tag{2.4}$$

where $\hat{\boldsymbol{\theta}}$ denotes the unit vector pointed towards the direction θ, and $k = w/c$ is the wave number associated with the frequency w. The vector $\mathbf{r}_m$ marks the coordinates of the mth sensor. We assume that the noise vectors $\mathbf{n}_k(w_j)$ are independent samples of stationary, zero mean circular complex Gaussian random process, with unknown covariance matrix $\sigma_n^2(w_j)\mathbf{I}$. The signal vectors $\mathbf{s}_k(w_j)$ are independent samples of stationary, zero mean circular complex Gaussian random process with unknown covariance matrix $\mathbf{R}_s(w_j)$. The noise process is assumed to be uncorrelated with the signal process. The wideband sources are assumed to share a common bandwidth. Due to the broadband nature of the sources, using coherent processing is advantageous as discussed in the previous section. Let $\mathbf{T}(w_j)$ denotes a transformation that maps the wideband array output from

frequency w_j to frequency w_0, so that the signal subspaces are aligned across the frequency bandwidth

$$\mathbf{T}(w_j)\mathbf{A}_{\boldsymbol{\theta}}(w_j) \cong \mathbf{A}_{\boldsymbol{\theta}}(w_0), \tag{2.5}$$

where w_j are within the bandwidth of the desired signal and w_0 is the focused frequency, i.e. $\mathbf{T}(w_j)$ focuses the signal subspaces $\mathbf{A}_{\boldsymbol{\theta}}(w_j)$ at frequencies $\{w_j\}$ onto the signal subspace $\mathbf{A}_{\boldsymbol{\theta}}(w_0)$. Following [37], we may construct the focused time-domain vector $\mathbf{y}_k(n)$ as

$$\mathbf{y}_k(n) = \sum_{j=1}^{J} \mathbf{T}(w_j)\mathbf{x}_k(w_j)e^{iw_j nT_s} \cong \mathbf{A}_{\boldsymbol{\theta}}(w_0)\mathbf{s}(n) + \widetilde{\mathbf{n}}(n), \tag{2.6}$$

where $\mathbf{s}(n)$ is the temporal vector of wideband unknown signals within the focused frequency band $[w_1 : w_J]$, T_s is the sampling frequency and $\widetilde{\mathbf{n}}(n)$ is the transformed noise. We note that the temporal focused vector $\mathbf{y}_k(n)$ has a narrowband array manifold while preserving the wideband spectral content of the signals. This allows the use of any narrowband adaptive beamformer matched to frequency w_0, such as the well known MVDR beamformer.

In this chapter we are interested in finding a focusing transformation $\mathbf{T}(w_j)$ which can handle DOA uncertainties while achieving the minimal mean-square focusing error at the true DOAs. To this end, we use the Bayesian approach in order to develop the focusing transformation. Let us employ a statistical model where the DOAs, $\{\theta_i\}_{i=1}^{P}$ are modelled as statistically independent random variables. We can now define and solve the Bayesian focusing problem for wideband arrays.

2.3 Bayesian Focusing Transformations (BFT)

In this section we consider the focusing problem with DOA uncertainties. We use a Bayesian model in order to define the optimal Minimum Mean Square Error (MMSE) focusing transformation $\mathbf{T}_{BFT}(w_j)$ as the solution to the following minimization problem

$$\mathbf{T}_{BFT}(w_j) = \arg\min_{\mathbf{T}(w_j)} E_{\boldsymbol{\theta}} \left\{ \|\mathbf{A}_{\boldsymbol{\theta}}(w_0) - \mathbf{T}(w_j)\mathbf{A}_{\boldsymbol{\theta}}(w_j)\|_F^2 \right\}, \tag{2.7}$$

where w_0 is the focusing frequency, $\|\cdot\|_F$ denotes the Frobenious norm, and $E_{\boldsymbol{\theta}}\{\cdot\}$ denotes the expectation over the statistical probability density distribution of the DOAs $\boldsymbol{\theta}$. Assuming $\{\theta_i\}_{i=1}^P$ are statistically independent random variables, it can be shown that

$$\begin{aligned} & E_{\boldsymbol{\theta}} \left\{ \|\mathbf{A}_{\boldsymbol{\theta}}(w_0) - \mathbf{T}(w_j)\mathbf{A}_{\boldsymbol{\theta}}(w_j)\|_F^2 \right\} \\ & = \int_{\theta=-\pi}^{\pi} d\theta \, \|\mathbf{a}_\theta(w_0) - \mathbf{T}(w_j)\mathbf{a}_\theta(w_j)\|^2 \sum_{i=1}^{P} f_{\theta_i}(\theta) \ , \end{aligned} \tag{2.8}$$

where $\|\cdot\|$ is the Euclidian norm and $f_{\theta_i}(\theta)$ denote the Probability Density Functions (PDFs) of the DOAs.

Proof of (2.8): Let us define $\mathcal{L}(w)$ as the function to be minimized

$$\begin{aligned} \mathcal{L}(w) &= E_{\boldsymbol{\theta}} \left\{ \|\mathbf{A}_{\boldsymbol{\theta}}(w_0) - \mathbf{T}(w)\mathbf{A}_{\boldsymbol{\theta}}(w)\|_F^2 \right\} \\ &= E_{\boldsymbol{\theta}} \left\{ \sum_{i=1}^{P} \|\mathbf{a}_{\theta i}(w_0) - \mathbf{T}(w)\mathbf{a}_{\theta i}(w)\|^2 \right\}, \end{aligned} \tag{2.9}$$

where $\|\cdot\|$ is the Euclidian norm. Assuming $\{\theta_i\}_{i=1}^{P}$ are statistically independent, (2.9) becomes

$$\begin{aligned}\mathcal{L}(w) &= \int d\theta_1 ... d\theta_P \; f_{\theta_1(\theta_1)} ... f_{\theta_P(\theta_P)} \cdot \\ &\sum_{i=1}^{P} \|\mathbf{a}_{\theta i}(w_0) - \mathbf{T}(w)\mathbf{a}_{\theta_i}(w)\|^2 \\ &= \sum_{i=1}^{P}\prod_{\substack{k=1\\k\neq i}}^{P}\underbrace{\int d\theta_k \; f_{\theta_k}(\theta_k)}_{=1} \cdot \\ &\int d\theta_i \; f_{\theta_i}(\theta_i) \, \|\mathbf{a}_{\theta i}(w_0) - \mathbf{T}(w)\mathbf{a}_{\theta i}(w)\|^2 \\ &= \int d\theta \, \|\mathbf{a}_{\theta}(w_0) - \mathbf{T}(w)\mathbf{a}_{\theta}(w)\|^2 \sum_{i=1}^{P} f_{\theta_i}(\theta_i) \; , \end{aligned} \tag{2.10}$$

which is exactly the form of the right hand side of (2.8). Defining

$$\rho^2(\theta) \triangleq \sum_{i=1}^{P} f_{\theta_i}(\theta), \tag{2.11}$$

and substituting (2.11) into the right-hand side of (2.8) yields the following integral to be minimized

$$\mathbf{T}_{BFT}(w_j) = \arg\min_{\mathbf{T}(w_j)} \int_{\theta=\,-\pi}^{\pi} d\theta \, \|\rho(\theta)(\mathbf{a}_{\theta}(w_0) - \mathbf{T}(w_j)\mathbf{a}_{\theta}(w_j))\|^2 \, . \tag{2.12}$$

Note that (2.12) is a generalized form which includes many focusing schemes as private cases. It reduces to the panoramic focusing scheme e.g. WINGS [22] by taking a uniform distribution i.e. $\rho(\theta) \equiv 1$. Taking $\rho(\theta) = \sum_i \delta(\theta - \hat{\theta}_i)$ yields the

directional focusing matrices originally proposed for wideband DOA estimation by Hung and Kaveh [9] which focuses at discrete angles taking to be the preliminary estimates of the DOAs $\left\{\hat{\theta}_i\right\}_{i=1}^{P}$. Note also that in (2.12) one may use either the a-priori PDFs as $f_{\theta_i}(\theta)$, or the a-posteriori PDFs. The first approach yields a data independent transformation, while the second approach requires estimation of the conditional PDFs from the data yielding a data dependent transformation. In Section 2.6 a time progressing algorithm employing the a-posteriori PDFs is proposed. In the following we solve (2.12) by deriving an accurate closed-form solution using a weighted extension of the WINGS [22] focusing approach. It is possible to solve (2.12) numerically, however, a closed form solution is preferable since it is more accurate.

2.4 BFT as a Weighted Extension of the WINGS

In this section we develop a closed form expression for a weighted extension of the WINGS focusing method, for the 2-D case, which incorporates an arbitrary angular weighting function $\rho(\theta)$. Finally, we show that the weighted extension is a closed form solution of (2.12).

Let us incorporate an arbitrary angular weighting function $\rho(\theta)$, in order to enhance the LS fit of the array manifold within a pre-selected angular region or to solve the Bayesian focusing problem (2.12). Let $\tilde{\varepsilon}_j$ be the weighted L_2 norm of

the focusing error $\mathbf{e}_\theta(w_j)$ (1.9)

$$\tilde{\varepsilon}_j^2 = \frac{1}{N}\int\limits_{\mathbf{\Gamma}} d\theta \left\|\rho(\theta)\mathbf{e}_\theta(w_j)\right\|^2 = \frac{1}{N}\int\limits_{\mathbf{\Gamma}} d\theta \left\|\rho(\theta)(\mathbf{a}_\theta(w_0) - \mathbf{T}(w_j)\mathbf{a}_\theta(w_j))\right\|^2, \quad (2.13)$$

where $\Gamma = \{-\pi, \pi\}$. In order to find the transformation minimizing (2.13) let us find $\mathbf{C}(w)$, the orthogonal decomposition of the product $\rho(\theta)\mathbf{a}_\theta(w)$

$$[\mathbf{C}(w)]_{mn} \equiv \int\limits_{\theta=\ -\pi}^{\pi} d\theta\rho(\theta)\left[(\mathbf{a}_\theta(w)\right]_m h_n(\theta). \quad (2.14)$$

where $\{h_n(\theta)\}$ is an orthogonal basis set in $\mathbf{L}_2(\Gamma)$, where Γ is the manifold of all the possible DOAs. In 2-D, we use the Fourier basis, i.e. $h_n(\theta) = \frac{1}{\sqrt{2\pi}}e^{-in\theta}$ (for more details see Sec.1.2.3 and [23]).

Let $\rho(\theta) = \sum_n \rho_n h_n(\theta)$ be the orthogonal decomposition of the angular weighting function $\rho(\theta)$, then substituting it into (2.14) and based on the wavefield modelling theory presented at Section 1.2, we may write

$$\begin{aligned}[\mathbf{C}(w)]_{mn} &= \int\limits_{\theta=\ -\pi}^{\pi} d\theta \sum_p \rho_p h_p(\theta) \sum_l \mathbf{G}_{ml}(w) h_l^*(\theta) h_n(\theta) \\ &= \sum_{p,l} \rho_p \mathbf{G}_{ml}(w) \int\limits_{\theta=\ -\pi}^{\pi} d\theta h_n(\theta) h_p(\theta) h_l^*(\theta). \end{aligned} \quad (2.15)$$

In the 2-D case the basis functions $h_n(\theta)$ are the Fourier functions and therefore

$$\int\limits_{\theta=\ -\pi}^{\pi} d\theta h_n(\theta) h_p(\theta) h_l^*(\theta) = \frac{1}{\sqrt{2\pi}}\delta_{n+p-l}, \quad (2.16)$$

which yields,

$$[\mathbf{C}(w)]_{mn} = \frac{1}{\sqrt{2\pi}} \sum_{p} \rho_p \mathbf{G}_{m,n+p}(w). \tag{2.17}$$

We now insert into (2.13) the orthogonal decomposition $\rho(\theta)\mathbf{a}_\theta(w) = \mathbf{C}(w)\mathbf{b}_\theta$ and get the following minimization integral

$$\tilde{\varepsilon}_j^2 = \frac{1}{N} \int_{\theta=-\pi}^{\pi} d\theta \left\| [\mathbf{C}(w_0) - \mathbf{T}(w_j)\mathbf{C}(w_j)]\mathbf{b}_\theta \right\|^2. \tag{2.18}$$

Using Parseval's identity we get

$$\tilde{\varepsilon}_j^2 = \frac{1}{N} \left\| [\mathbf{C}(w_0) - \mathbf{T}(w_j)\mathbf{C}(w_j)] \right\|_F^2. \tag{2.19}$$

Thus, the weighted WINGS transformation minimizing $\tilde{\varepsilon}_j$ is given by the LS solution of (2.19)

$$\mathbf{T}(w_j) = \mathbf{C}(w_0)\mathbf{C}^\dagger(w_j). \tag{2.20}$$

Since (2.13) has exactly the same form as (2.12), we get the closed form expression for the MMSE optimal BFT

$$\mathbf{T}_{BFT}(w_j) = \mathbf{C}(w_0, \rho(\theta))\mathbf{C}^\dagger(w_j, \rho(\theta)), \tag{2.21}$$

where $\rho(\theta)$ is given by (2.11).

In the following section we numerically evaluate the focusing error of the BFT, and compare it to that of the WINGS, WKFT, and RSS methods which were reviewed in Section 1.2.

2.5 Numerical Study of the Focusing Error in the Presence of DOA Uncertainties

In this section, we conduct a numerical study of the focusing errors of the presented focusing methods in the presence of DOAs uncertainties. We compare the performance of four focusing transformations: The BFT representing the Bayesian focusing approach, WINGS representing the panoramic focusing approach, the WKFT [7] and the unitary transformation RSS [9] representing the directional focusing approach, which focuses a discrete set of preliminary DOA estimates. In the following example, we take two circular complex Gaussian wideband acoustic sources propagating towards a linear array of N=20 sensors in velocity of 1500 m/sec. The simulation results were obtained by averaging over 100 independent Monte-Carlo runs. We simulate the actual DOA errors as Gaussian random variables with a standard deviation on the order of a half of the 3dB beamwidth, and mean value of $\boldsymbol{\theta} = [70°, 105°]$ where 90° is the broadside direction. The desired signal is the one arriving from 105°. The Signal to Interference Ratio (SIR) is set at a fixed value of -20dB. The bandwidth of the sources is 600Hz taken around $f_c = 1500$Hz and the spectrum is taken to be flat in the relevant bandwidth. The sampling frequency is 4800Hz. The focusing frequency is $f_0 = 1500$Hz. The observation time T is taken as 10 seconds and divided into $K = 46$ snapshots. Each snapshot of data is transformed to the frequency domain using a Fast Fourier Transform(FFT) of 1024 bins yielding $J = 129$ frequency bins in the relevant bandwidth. The spacing between two adjacent sensors is $d = \frac{\lambda_{\min}}{2}$, where $\lambda_{\min}$

corresponds to the highest frequency of the bandwidth. For the BFT, we take the weighting function $\rho^2(\theta)$ (2.11), to be a sum of Gaussian densities centered around the assumed DOAs

$$\rho^2(\theta) = \frac{1}{\sqrt{2\pi\sigma_1^2}} \exp(-\frac{(\theta-\theta_1)^2}{2\sigma_1^2}) + \frac{1}{\sqrt{2\pi\sigma_2^2}} \exp(-\frac{(\theta-\theta_2)^2}{2\sigma_2^2}) \tag{2.22}$$

Where θ_1 and θ_2 are the assumed DOAs of the sources and the standard deviations $\sigma_1 = 1.27$ and $\sigma_2 = 1.25$ which are approximately on the order of a quarter of the 3dB beamwidth of the array at θ_1 and θ_2, respectively. In the WKFT and RSS methods we add 2 auxiliary directions for each assumed DOA in order to increase the robustness to DOAs uncertainties. The auxiliary directions were added at a quarter of the 3dB beamwidth from the assumed DOAs.

Fig.2.1 shows the focusing transformation error $\|\mathbf{e}_\theta(w_j)\|^2$ (1.9) versus frequency averaged over 100 Monte-Carlo runs and summed over all the true source directions, for the BFT, WINGS, WKFT and RSS methods. It can be seen that the BFT method has the lowest focusing error along the entire bandwidth. Both WKFT and RSS focusing methods introduce a high focusing error since they require preliminary DOAs estimates. In the WINGS method, we see that large errors occur at frequencies below the focusing frequency. This is expected since WINGS is an interpolation based focusing method, in which focusing is equivalent to spatial interpolation [18] of the array. Interpolating from a low frequency to a higher one, is equivalent to extrapolating the array beyond its physical length, thus, yielding high focusing errors. One can reduce the WINGS transformation error by focusing to the lowest frequency of the bandwidth. However, this will

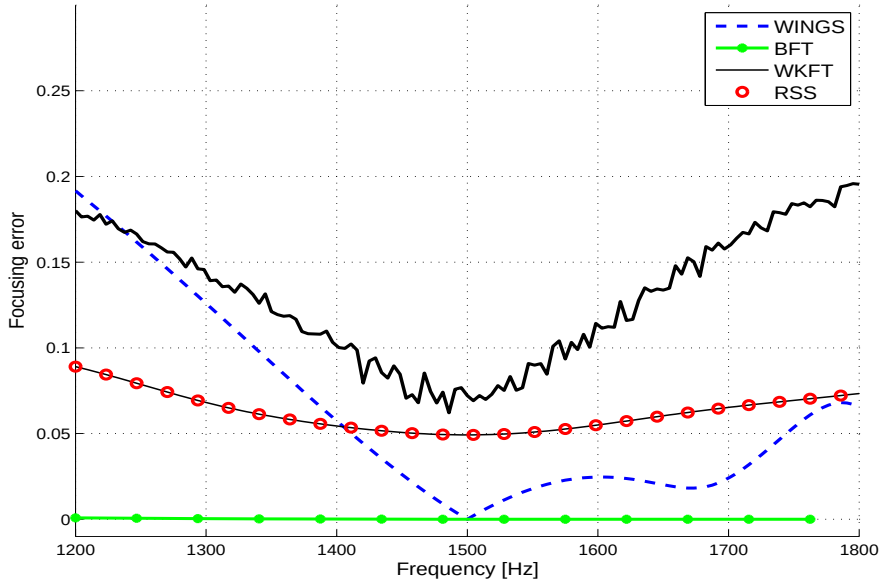

Figure 2.1: Focusing transformation error for BFT, WINGS, WKFT and RSS matrices versus frequency for the case of two sources and DOA uncertainties

reduce the effective aperture of the focused array, thus reducing the spatial resolution of the array. In the literature there are several papers dealing with the issue of choosing the optimal focusing frequency (e.g. [38,39]). However, optimizing the focusing frequency is beyond the scope of this work.

Fig.2.2 shows the error versus angle due to focusing from frequency $f = 1350$Hz to frequency f_0 for the BFT, WINGS WKFT and RSS methods and DOAs error of approximately 3 degrees for each source. The true DOAs are marked on the same plot by the diamonds. It can be seen that the WINGS method has a roughly equi-ripple focusing error for all the directions. This is expected because WINGS is an interpolated based panoramic focusing method which does not depends on the DOAs. BFT, RSS and WKFT have a high focusing error in directions which

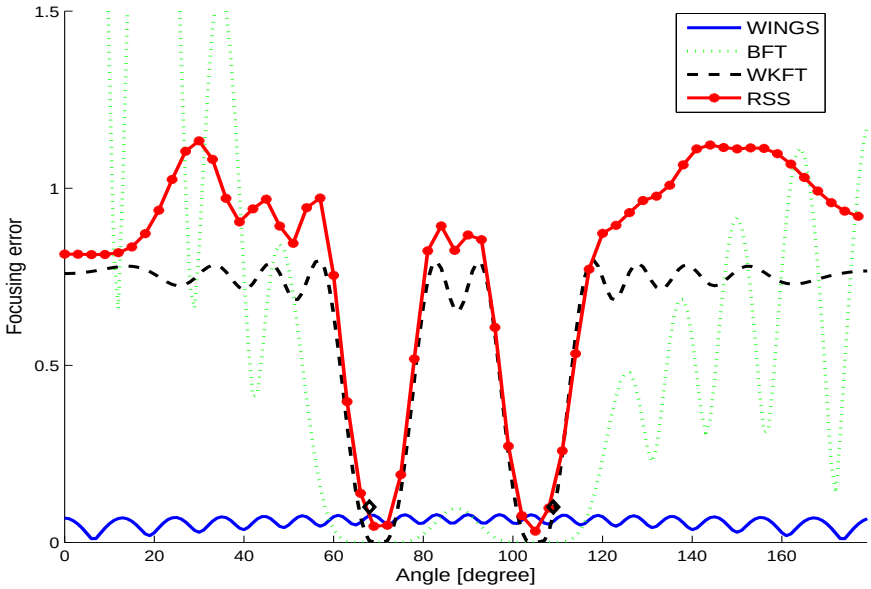

Figure 2.2: Error versus angle due to focusing from $f = 1350$Hz to f_0 for BFT, WINGS, WKFT and RSS for the case of two sources and DOA uncertainties.

are distant from the assumed DOAs, and a low focusing error in directions which are close to the assumed DOAs. It can be seen that BFT is significantly more robust to DOA uncertainties since it has a low focusing error over a wide range of angles.

Fig.2.3 shows the focusing error as a function of the sensor index in the desired source direction averaged over the entire bandwidth, for the BFT, WINGS, RSS and WKFT focusing methods, for a DOA error of approximately 3 degrees. We can see that BFT has the smallest focusing error along the sensors while WKFT and RSS has the largest errors. It can be seen that the error at the edges of the array for the BFT and WINGS methods is significantly larger than the error in the center of the array. This can be explained due to the fact that both methods

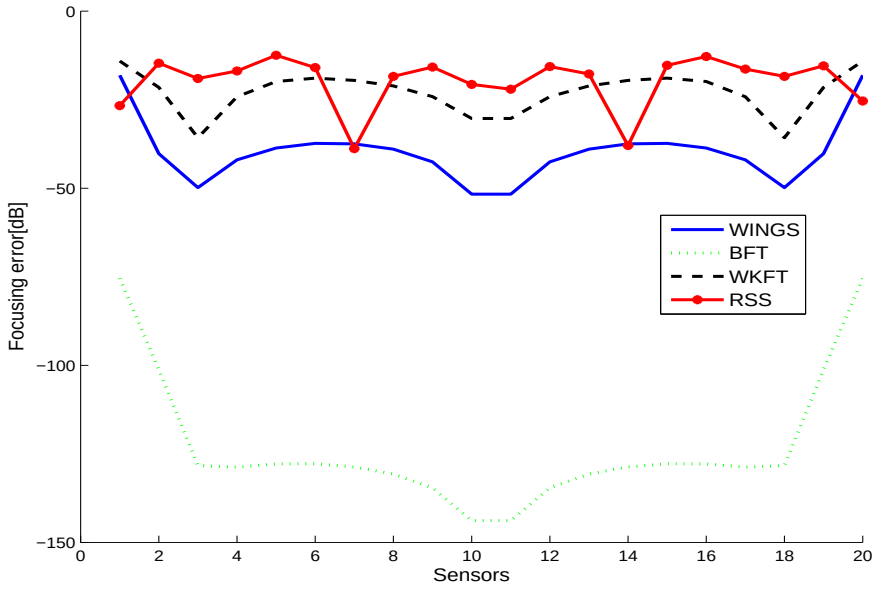

Figure 2.3: Average Focusing error in the desired source direction for BFT, WINGS, WKFT and RSS versus sensors for the case of two sources and DOA uncertainties

are based on interpolation which require to extrapolating the array beyond its physical length, thus, yielding high focusing errors at the edges of the array.

The numerical results show that the BFT introduces a relatively lower focusing error than that of the other focusing methods, thus, it provides more robust and accurate focusing operation. The focusing error of the WINGS is significantly high at low frequencies because it is an interpolation based method, however, it is not sensitive to DOAs uncertainties. In both WKFT and RSS focusing methods, the focusing error is expected to reduce as the uncertainties in the DOAs decrease. In fig. 2.4 the focusing error of WKFT and RSS methods is presented for the case of perfect knowledge of the DOAs. It can be seen that the error was reduces

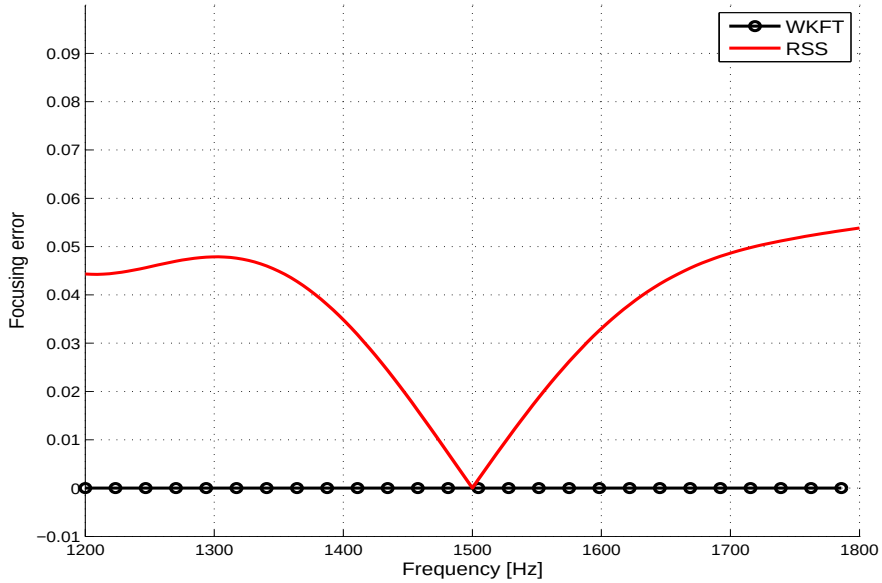

Figure 2.4: Focusing transformation error for WKFT and RSS versus frequency for the case of two sources and perfect knowledge of the DOAs

significantly, especially in the WKFT focusing method. In the RSS, the focusing error is also reduced, however, still non negligible because of the unitary constraint. This implies that RSS is less suitable to coherent beamforming processing than the WKFT method. In the following, we will see that the performance of the RSS is good for DF applications when employing subspace based DF algorithms.

2.6 Time Progressing Algorithm

In this section we present a time progressing algorithm which is based on the proposed Bayesian focusing approach. The BFT assumes that the PDFs of the DOAs are available. However, in practice we need to estimate the a-posteriori

PDFs of the DOAs. Under the assumption of a Gaussian model for the DOAs, we have to estimate the first two moments of each DOA. The conditional mean of θ_i is approximated by $\hat{\theta}_{i\_DF}$ which is the estimate of the DF algorithm such as MUSIC. The standard deviation is taken to be a quarter of the 3dB beamwidth of the array. A block diagram of the proposed algorithm is given in figure 2.5. Each T seconds of data are divided into K snapshots, on which, a Bayesian focusing transformation is applied and yields the focused vector. The design of the focusing transformation uses the estimated aposteriori PDFs from the previous T seconds, while in the first T seconds, the algorithm uses $\rho(\theta) \equiv 1$. The focused temporal vectors $\{\mathbf{y}_k\}_{k=1}^{K}$are used as inputs to the focused MVDR beamformer and for updating the estimation of the conditional PDFs.

Note that for the WKFT and RSS focusing methods, a similar algorithm can be applied, at each time step the DOAs vector will be estimated by the DF algorithm from the focused data and will be used as input to the focusing stage in the next time step.

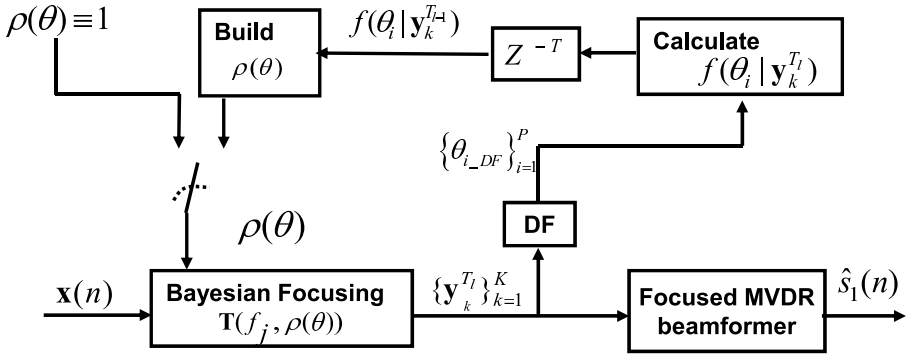

Figure 2.5: Block diagram of the Bayesian focused MVDR beamformer time progressing algorithm.

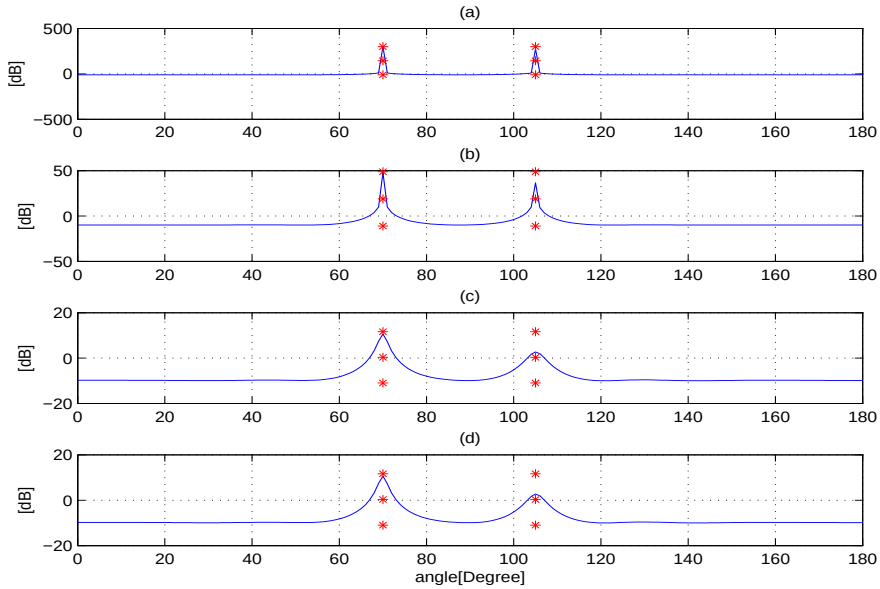

Figure 2.6: DOAs estimation by the MUSIC algorithm for the various focusing methods. (a)WKFT, (b)RSS, (c)WINGS, (d)BFT

In Fig. 2.6, the output of the MUSIC algorithm is presented for all the focusing methods. In each of the true DOAs there is a peak in the MUSIC spectrum. We can see that the WKFT and RSS methods produce narrower and stronger peaks than the WINGS and BFT. The relatively accurate DOAs estimations of the RSS focusing method in spite of its high focusing error is surprising. The reason for that is because RSS focusing method preserves the signal subspace before and after the focusing operation [15]. The MUSIC algorithm is a subspace based algorithm and hence does not influenced by the focusing error. Therefore, the RSS is a focusing method which suitable for subspace based DF algorithms such as MUSIC and less suitable to beamforming applications. So, in subsequent chapters we concentrate only in WINGS, WKFT and BFT focusing methods.

2.7 Summary

We have proposed and investigated a Bayesian approach for focusing transformation design, which takes into account the statistical uncertainties in the DOAs during the focusing process. The proposed Bayesian focusing approach is a compromise between the directional focusing approaches which require preliminary DOA estimates, and the panoramic focusing approaches which are based on spatial interpolation not requiring any DOA estimates. We showed that the solution to the Bayesian focusing problem is equivalent to finding the weighted WINGS focusing transformation and supply a closed form expression for the BFT transformation. The solution to the Bayesian focusing problem yields an optimal MMSE focusing transformation and consequently an improved focused beamformer with better AG, as will be shown in next chapters.

Simulation results have illustrated the very low focusing error of the proposed BFT method for the multi-source case in the presence of DOA uncertainties compared to that of the WINGS, RSS and WKFT focusing methods.

A time progressing algorithm was proposed which consists of two stages, the first performs DF on the focused vector and the second stage is the focused beamformer algorithm. The DF stage is required for the BFT, RSS, and WKFT focusing methods.

In the next chapter we propose a robust version of the focused MVDR beamformer and conduct a numerical study of the performance of the various focusing methods under DOAs uncertainties scenarios.

Chapter 3

Robust Adaptive Focused MVDR Beamformer and Performance Analysis

3.1 Introduction

In the previous chapter we derive a Bayesian focusing transformation which is an optimal MMSE transformation for the case of DOAs uncertainties. The focusing transformation operates on the received wideband data vector yielding a focused data vector $\mathbf{y}_k(n)$ (2.6). On $\mathbf{y}_k(n)$, there can be applied any narrowband adaptive beamforming algorithm such as the well-known Capon beamformer [30] ,also referred to as the Minimum Variance Distortionless Response (MVDR) beamformer. The MVDR has a better resolution capability and an improved interference rejection capabilities than that of the conventional beamformer, provided that the array

response to the Signal of Interest (SOI) is perfectly known. However, in practice, there are some inaccuracies due to array calibration errors, DOA errors [31], and also the sample covariance matrix estimation errors have a significant affect [33]. In the focused MVDR beamformer, the focusing error also comes into play and may deteriorate the performance. In order to reduce the various sensitivities of the MVDR beamformer, a robust beamforming scheme must be used.

In this chapter, we derive and employ an extension of the diagonal loading method for the coherent wideband case. We refer to this solution as the Q-loading solution in which we add a scaled matrix Q to the covariance matrix before inversion, where the matrix Q depends on the focusing transformations. Via numerical simulations, we find this solution to yield a significant improvement in the performance and robustness against mismatch and focusing errors.

In order to conduct a comparative performance study of the various focusing methods on a robust beamformer scheme, we develop an analytic expression for the Array Gain (AG) of the robust focused MVDR beamformer. We use the analytic expression and numerical Monte-Carlo simulations in order to investigate the influence of the focusing error of the BFT on the performance of the focused beamformer and compare it to that of the other focusing methods.

This chapter is organized as follows: In Section 3.2 we derive the robust focused Q-loaded MVDR beamformer. In Section 3.3 The analytic AG of the focused Q-loaded MVDR beamformer is derived. In Section 3.4 we present some simulation examples of our robust BFT focused MVDR beamformer and compare its performance to other focusing methods. Finally, we summarize this chapter in

Section 3.5.

3.2 Robust MVDR Focused Beamformer by Q-Loading

In this section we treat the issue of robust wideband focused MVDR beamformers, i.e. reducing the sensitivity to inaccurate knowledge of the array steering vector in the direction of the desired source, such as gain, phase calibration errors, source direction errors, and sample covariance matrix estimation errors.

The MVDR beamformer is known to have superior resolution and interference rejection capabilities, provided that the array steering vector corresponding to the SOI is accurately known. In practice, it is often the case, due to array calibration errors and inaccurate knowledge of the source direction, that the performance of the MVDR beamformer may deteriorate below that of the conventional beamformers [31]. Furthermore, the MVDR-SMI implementation is sensitive to estimation errors in the sample covariance matrix [33]. In the coherent wideband case, the focused MVDR beamformer will exhibit an additional sensitivity to the focusing errors. Many robust schemes constraint the Euclidian norm of the beamformer coefficient vector, thus decreasing the sensitivity to various modelling errors.

Diagonal loading has been a popular approach to improve the robustness of the MVDR beamformer [1, 33–35]. It is derived by imposing an additional quadratic constraint either on the Euclidian norm of the weight vector itself or on its difference from the nominal weight vector (for more details see Section 1.2.5).

Many of the robust schemes statistically model the various inaccuracies as random spatially uncorrelated additive noise at the input of the adaptive beamformer. Under this assumption the noise power at the narrowband beamformer output is

$$n_{out} = \sigma_n^2(w) \left\| \mathbf{w}_\theta(w) \right\|^2 \tag{3.1}$$

where $\sigma_n^2(w)$ in the input noise power and $\mathbf{w}_\theta(w)$ in the MVDR weight vector. Thus, limiting the norm of $\mathbf{w}_\theta(w)$, is equivalent to limiting the white noise gain. In the case of the focused beamformer, the output noise power is given by

$$\sigma_{n_{out}}^2 = \sigma_n^2 (\mathbf{w}_\theta^f)^H \left(\frac{1}{J} \sum_{l=1}^{J} \mathbf{T}(w_l) \mathbf{T}^H(w_l) \right) \mathbf{w}_\theta^f, \tag{3.2}$$

where we assumed the noise spectrum to be frequency independent, i.e. $\sigma_n^2(w) = \sigma_n^2, \forall w$. Thus, limiting the white noise gain yields the following quadratic constraint

$$(\mathbf{w}_\theta^f)^H \mathbf{Q} \mathbf{w}_\theta^f \leq T_0, \tag{3.3}$$

where we define

$$\mathbf{Q} \triangleq \frac{1}{J} \sum_{l=1}^{J} \mathbf{T}(w_l) \mathbf{T}^H(w_l) \tag{3.4}$$

and T_0 is a design parameter. The robust focused MVDR beamformer optimization problem can be written as

$$\min_{\mathbf{w}_\theta^f} (\mathbf{w}_\theta^f)^H \mathbf{R}_x^f \mathbf{w}_\theta^f, \tag{3.5a}$$

subject to the distortionless constraint,

$$(\mathbf{w}_\theta^f)^H \mathbf{a}_\theta(w_0) = 1, \tag{3.5b}$$

and the quadratic constraint,

$$(\mathbf{w}_\theta^f)^H \mathbf{Q} \mathbf{w}_\theta^f \leq T_0. \tag{3.5c}$$

It can be shown that the solution to (3.5) is given by (see Appendix A.1)

$$\mathbf{w}_\theta^{f,QL} = \frac{\left(\mathbf{R}_x^f + \beta\mathbf{Q}\right)^{-1} \mathbf{a}_\theta(w_0)}{\mathbf{a}_\theta^H(w_0) \left(\mathbf{R}_x^f + \beta\mathbf{Q}\right)^{-1} \mathbf{a}_\theta(w_0)}, \tag{3.6}$$

where β is the Lagrange multiplier which is determined in such a way that the quadratic constraint is satisfied. Note that in (3.6) the loading term $\beta\mathbf{Q}$ is not a diagonal matrix as in the narrowband case. Thus, for the focused MVDR case we use the notation Q-loading.

In order to find β analytically, one has to solve a set of secular equations ([32],ch.12). Instead of solving them directly, it can be shown that the quadratic norm $\mathbf{w}^H\mathbf{Q}\mathbf{w}$ is a monotonic decreasing function of β (see Appendix A.2). Thus, we can find β iteratively starting from $\beta = 0$ and increasing it until the quadratic constraint is satisfied.

The lower bound for T_0 can be calculated by taking β to the infinity which yields

$$T_{0\_\min} = \lim_{\beta\to\infty} \mathbf{w}^H\mathbf{Q}\mathbf{w} = \frac{\mathbf{1}}{\mathbf{a}_\theta^H(w_0)\mathbf{Q}^{-1}\mathbf{a}_\theta(w_0)} \tag{3.7}$$

In this case the beamformer becomes independent of the covariance matrix $\mathbf{R}_x^f$ as in the conventional beamformer. For the case of unitary focusing transformation, $\mathbf{Q}$ is reduced to the unit matrix and the lower bound for T_0 reduces to the white noise gain of the conventional beamformer. In the following section, we derive an analytic expression for the AG of the focused Q-loaded MVDR beamformer and compare it to the simulative AG based on Monte-Carlo runs of the SMI implementation. We compare the performance of various focusing methods and study their dependence on the accuracy of the focusing transformation.

3.3 Analytic AG

In this section, we derive an analytic expression for the AG of the Q-loaded MVDR focused beamformer as a function of the focusing transformations. The focusing process introduces a frequency dependent transformation error which affects the performance of the MVDR focused beamformer. The analytic expression will be used to evaluate the performance of the focused beamformer for the various focusing methods. The expression developed here is the asymptotic limit to the performance since it involves the asymptotic covariance matrix of the data and not an estimated sample version of it. The covariance matrix of the received focused data vector $\mathbf{y}_k(n)$ (2.6) is given by

$$\begin{aligned}\mathbf{R}_x^f &= E\mathbf{y}_k(n)\mathbf{y}_k^H(n) \\ &= E\sum_{j,l=1}^{J}\mathbf{T}(w_j)\mathbf{x}_k(w_j)e^{iw_jnT_s}(\mathbf{T}(w_l)\mathbf{x}_k(w_l)e^{iw_lnT_s})^H, \end{aligned} \tag{3.8}$$

assuming different frequencies to be statistically independent, (3.8) becomes

$$\mathbf{R}_x^f = \sum_{j=1}^{J} \mathbf{T}(w_j) E\left\{\mathbf{x}_k(w_j)\mathbf{x}_k^H(w_j)\right\}\mathbf{T}^H(w_j) \triangleq \sum_{j=1}^{J} \mathbf{T}(w_j)\mathbf{R}_x(w_j)\mathbf{T}^H(w_j). \quad (3.9)$$

For simplicity, we assume uncorrelated sources. Taking $s_1(t)$ to be the desired signal propagating from θ_1. Let P_{s_1}, P_i, P_n to be the power of the desired signal, the interferences signals, and the noise, respectively

$$\begin{aligned} P_{s_1} &= \sum_{j=1}^{J} \sigma_{s_1}^2(w_j) \\ P_i &= \sum_{p=2}^{P}\sum_{j=1}^{J} \sigma_{s_p}^2(w_j) \\ P_n &= \sum_{j=1}^{J} \sigma_n^2(w_j). \end{aligned} \quad (3.10)$$

Let us define

$$\mathbf{a}_\theta^f(w_j) = \mathbf{T}(w_j)\mathbf{a}_\theta(w_j), \quad (3.11)$$

to be the focused steering vector in direction θ and frequency w_j.

Let also $P_{s_1\_out}, P_{i\_out}, P_{n\_out}$ denote the output power of the desired signal, the interferences, and the noise, respectively, then one can see that

$$P_{s_1\_out} = \sum_{j=1}^{J} \sigma_{s_1}^2(w_j) \left|(\mathbf{w}_{\theta_1}^{f,QL})^H \mathbf{a}_{\theta_1}^f(w_j)\right|^2, \quad (3.12)$$

$$P_{i\_out} = \sum_{p=2}^{P}\sum_{j=1}^{J}\sigma_{s_p}^2(w_j)\left|(\mathbf{w}_{\theta_1}^{f,QL})^H\mathbf{a}_{\theta_p}^f(w_j)\right|^2, \tag{3.13}$$

$$P_{n\_out} = (\mathbf{w}_{\theta_1}^{f,QL})^H\left(\sum_{j=1}^{J}\mathbf{T}(w_j)\mathbf{R}_n(w_j)\mathbf{T}^H(w_j)\right)\mathbf{w}_{\theta_1}^{f,QL}, \tag{3.14}$$

where $\mathbf{R}_n(w_j)$ is the noise covariance matrix. Assume θ_1 is known, $\mathbf{w}_{\theta_1}^{f,QL}$ is the Q-loaded focused MVDR weight vector

$$\mathbf{w}_{\theta_1}^{f,QL} = \frac{(\mathbf{R}_x^f + \beta\mathbf{Q})^{-1}\mathbf{a}_{\theta_1}(w_0)}{\mathbf{a}_{\theta_1}^H(w_0)(\mathbf{R}_x^f + \beta\mathbf{Q})^{-1}\mathbf{a}_{\theta_1}(w_0)}, \tag{3.15}$$

Defining the $SINR_{in}, SINR_{out}$ to be the Signal to Interference plus Noise Ratio(SINR) at the input and output of the beamformer, respectively

$$\begin{aligned} SINR_{in} &= \frac{P_{s_1}}{P_i + P_n} \\ SINR_{out} &= \frac{P_{s_1\_out}}{P_{i\_out} + P_{n\_out}}, \end{aligned} \tag{3.16}$$

then, the AG is the ratio between $SINR_{out}$ and $SINR_{in}$. Substituting (3.15) into (3.12)- (3.14), yields

$$AG = \frac{\mathbf{a}_{\theta_1}^H(w_0)(\tilde{\mathbf{R}}_x^f)^{-1}\left(\sum_{j=1}^{J}\sigma_{s_1}^2(w_j)\mathbf{a}_{\theta_1}^f(w_j)(\mathbf{a}_{\theta_1}^f(w_j))^H\right)(\tilde{\mathbf{R}}_x^f)^{-1}\mathbf{a}_{\theta_1}(w_0)}{\mathbf{a}_{\theta_1}^H(w_0)(\tilde{\mathbf{R}}_x^f)^{-1}\left(\sum_{j=1}^{J}\left[\sum_{p=2}^{P}\sigma_{s_p}^2(w_j)\mathbf{a}_{\theta_p}^f(w_j)(\mathbf{a}_{\theta_p}^f(w_j))^H + \mathbf{R}_n^f(w_j)\right]\right)(\tilde{\mathbf{R}}_x^f)^{-1}\mathbf{a}_{\theta_1}(w_0)\cdot SINR_{in}} \tag{3.17}$$

where:

$$SINR_{in} = \frac{\sum_{j=1}^{J} \sigma_{s_1}^2(w_j)}{\sum_{p=2}^{P}\sum_{j=1}^{J} \sigma_{s_p}^2(w_j) + \sum_{j=1}^{J} \sigma_n^2(w_j)}, \tag{3.18}$$

$$\tilde{\mathbf{R}}_x^f = \mathbf{R}_x^f + \beta \mathbf{Q}, \tag{3.19}$$

and

$$\mathbf{R}_n^f(w_j) = \mathbf{T}(w_j)\mathbf{R}_n(w_j)\mathbf{T}^H(w_j), \tag{3.20}$$

is the focused noise covariance matrix.

In order to calculate $\mathbf{R}_x^f$ using (3.9), $\mathbf{R}_x(w_j)$ should be evaluated. In the case of uncorrelated sources and spatially uncorrelated noise (i.e. $\mathbf{R}_n(w_j) = \sigma_n^2(w_j)\mathbf{I}$, we get

$$\mathbf{R}_x(w_j) = \sum_{p=1}^{P} \sigma_{s_p}^2(w_j)\mathbf{a}_{\theta_p}(w_0)\mathbf{a}_{\theta_p}^H(w_0) + \sigma_n^2(w_j)\mathbf{I} \tag{3.21}$$

In the following sections, we conduct a numerical performance analysis based on the asymptotic expression (3.17). We will first demonstrate the performance in the presence of DOA uncertainties in order to illustrate the advantage of the BFT over other focusing approaches. Later, we conduct a numerical and analytic study of the sensitivity to focusing transformation errors at high SNR values.

3.4 Numerical Study for the Case of DOAs Uncertainties

In this section we evaluate the performance of the Q-loaded SMI-MVDR beamformer for three of the focusing methods discussed in the previous chapter: BFT, WINGS and WKFT. For Q-loading, we set $T_0 = 0.25$ which is five times the norm of the conventional beamformer. All the rest of the simulation parameters are identical to those of Section 2.5. In Fig.3.1(a) and Fig.3.1(b) we plot the asymptotic and the simulative AG versus SNR for BFT, WINGS and WKFT methods for the coherent MVDR beamformer with and without Q-loading, respectively. The superior performance of the BFT over that of the WINGS and WKFT in both analytic and simulative curves, is expected due to its low focusing error. The performance difference is especially large in the analytic AG curves and increases with SNR, while the simulative curves exhibits a smaller yet still significant performance difference. The significant difference between the analytic and simulative AG especially in the BFT method is due to the fact that in the analytic calculation we use the asymptotic focused covariance matrix (3.9) while in the simulation we use the SMI estimation version of it (1.18) computed by averaging over $K = 46$ snapshots. In Fig.3.2 the AG of the BFT focused beamformer without Q-loading is plotted for various values of K. The analytic AG (3.17) which is considered to be the asymptotic AG is also plotted and we can see that as K increases, the simulative curves approach the analytic curve.

Finally, comparing Fig.3.1(a) and Fig.3.1(b) we see that a significant improve-

ment of the AG is achieved by appropriate Q-loading of the covariance matrix. We see that the Q-loading effectively reduces the sensitivity of the MVDR beamformer to the focusing errors of the different methods as well as to the SMI estimation errors and DOAs uncertainties. In Fig.3.3 the AG versus ISR is plotted for SNR value of 40dB. The BFT exhibits superior performance for all SIR values.

Let us now examine a single source example. In Fig.3.4(a) and Fig.3.4(b) we plot the asymptotic and the simulative AG versus SNR for BFT, WINGS and WKFT methods for the case of one source and DOA uncertainty for the MVDR focused beamformer with and without Q-loading, respectively. First, we note the significant improvement in the AG achieved by the Q-loading. Without Q-loading the AG decreases to values below -40dB, while with Q-loading we observe a slight decrease in the AG for mid range SNR values. However, as the SNR increases the Q-loading term become significant and the AG converges to a steady value , which depends on the focusing errors. The comparison of the performance of the different focussing methods for the single source case given in Fig.3.4 shows a significant advantage of the BFT over that of WINGS, while WKFT exhibits relatively good performance. We see that in this case WKFT has an advantage over the BFT in the simulative curve. While in the analytic curve, BFT achieves a good AG over the entire range of the SNR values while WKFT achieves the best AG at low SNR values. From both Fig.3.4(a) and Fig.3.4(b) it can be seen that WKFT achieves an AG about 1dB higher then that of the BFT in the region of the low SNR values. The reason for this is that in both BFT and WINGS methods, the beamwidth is wider than the beamwidth in the WKFT method as can be seen in Fig.3.5(a)

where the beampatterns of all the methods are plotted for the single source case and for low SNR value of -10dB. In order to understand this phenomena, we examine in Fig.3.5(b) the corresponding magnitudes of the adaptive coefficients vector. In BFT and WINGS which are considered to be an interpolation based approaches, it can be seen that the "effective" array is reduced to only 16 sensors while the physical array was of 20 sensors. Since the single source AG is roughly $10\log_{10} N$ where N is the number of sensors, we get a difference of approximately 1dB in the AG.

The results presented in this section demonstrated the superiority of the BFT over the WINGS and WKFT focusing methods in multi-source scenarios in the presence of DOA uncertainties. We also demonstrated the efficiency of the Q-loading procedure introduced in section 3.2 in improving the robustness of the focused MVDR beamformer to focusing errors and to the SMI implementation errors.

3.5 Summary

In this chapter, we first treated the important issue of reducing the beamformers' sensitivity to focusing errors, and to other modelling errors such as gain and phase calibration errors, source direction errors, and covariance matrix estimation errors. We derived the Q-loaded wideband focused SMI-MVDR beamformer, which is a practical robust MVDR version for the focused beamformer. The Q-loaded focused MVDR beamformer employs a generalized *transformation-dependent* loading of the sample covariance matrix, thus taking into account the focusing process

in the robust version. This yields superior robustness compared to that of the popular diagonal loading method. We note that the Q-loaded MVDR beamformer is a *transformation-dependent* process, which may be applied after any arbitrary focusing scheme for robust focused beamforming.

To evaluate the performance of the proposed BFT method and other focusing methods we derived an analytic expression of the asymptotic AG for the SMI-implementation of the focused Q-loaded MVDR beamformer. Simulation results have illustrated the superiority of the proposed BFT method for the multi-source case in DOA uncertainties conditions compared to that of the WINGS and WKFT focusing methods. This is attributable to the low focusing error of the BFT across the entire bandwidth, which yields more accurate focused data. In the single source case, WKFT exhibits relatively good performance because of its narrower beamwidth compared to other focusing methods. The significant improvement in the performance and robustness of the focused Q-loaded MVDR beamformer with respect to that of the un-loaded MVDR was also demonstrated.

An eminent point arising from both Fig.3.1(b) and Fig.3.4(b) is the degradation in the analytic performance of WINGS and WKFT methods as the SNR increased. In the following chapter, we investigate this degradation and show analytically that it occurs due to the focusing error in the desired source direction. In order to reduce this sensitivity, we propose and study two robust methods for coherent focused wideband MVDR beamforming.

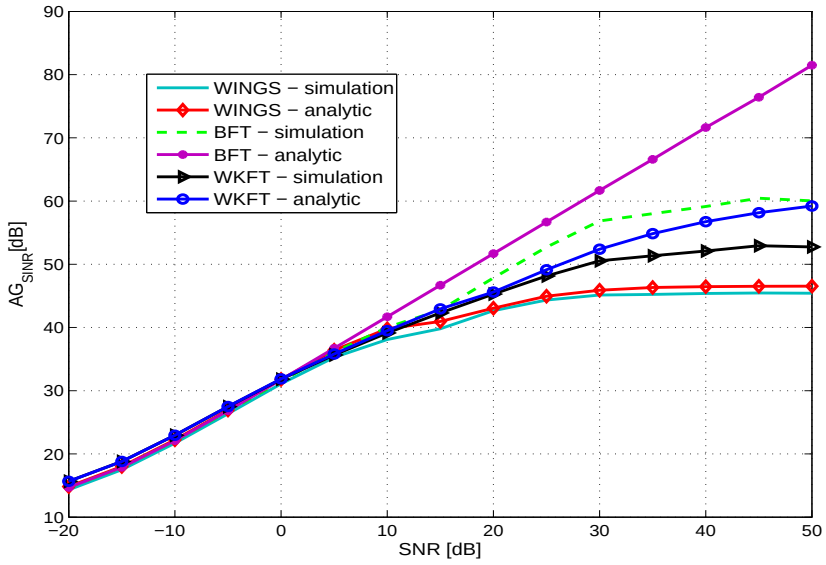

(a)

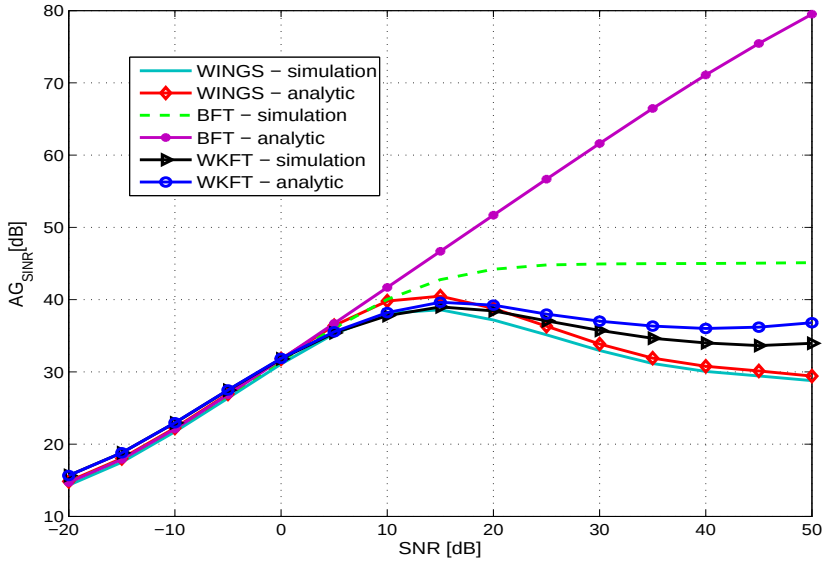

(b)

Figure 3.1: Array gain versus SNR for BFT, WINGS and WKFT for the case of two sources and DOA uncertainties. (a) With Q-loading, (b) Without Q-loading

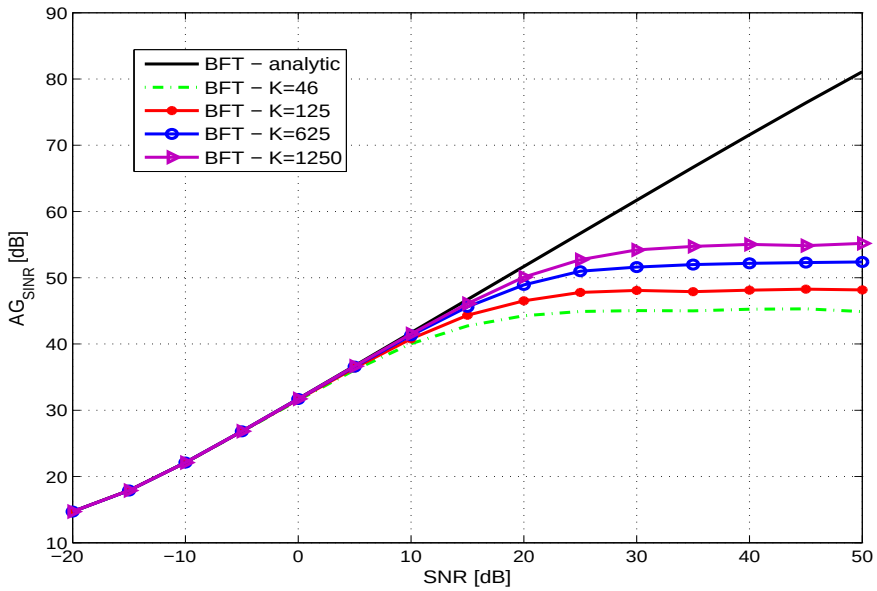

Figure 3.2: AG versus SNR of BFT for various values of the number of the snapshots K for the case of two sources with DOA uncertainties and without Q-loading.

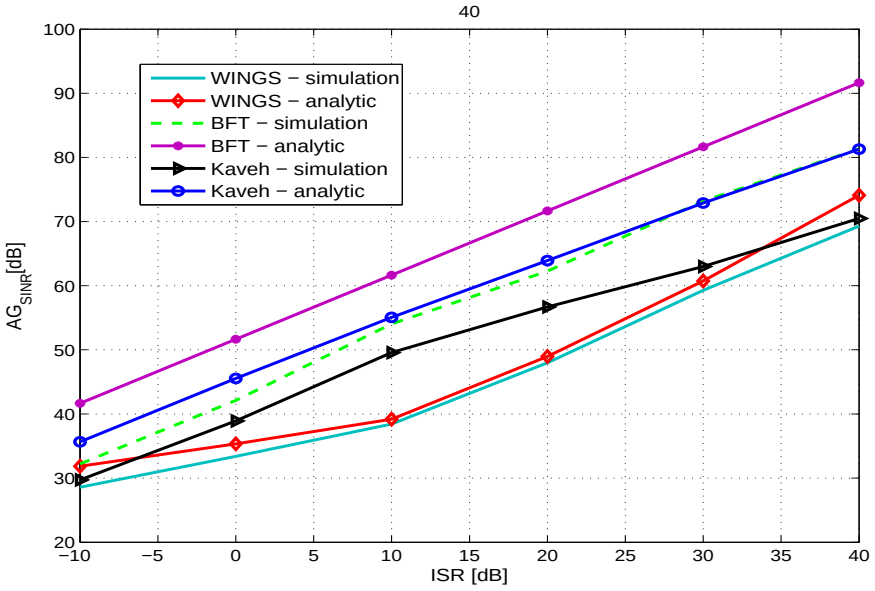

Figure 3.3: Array gain versus ISR for $SNR = -10$dB. Two sources and DOA uncertainties and using Q-loading.

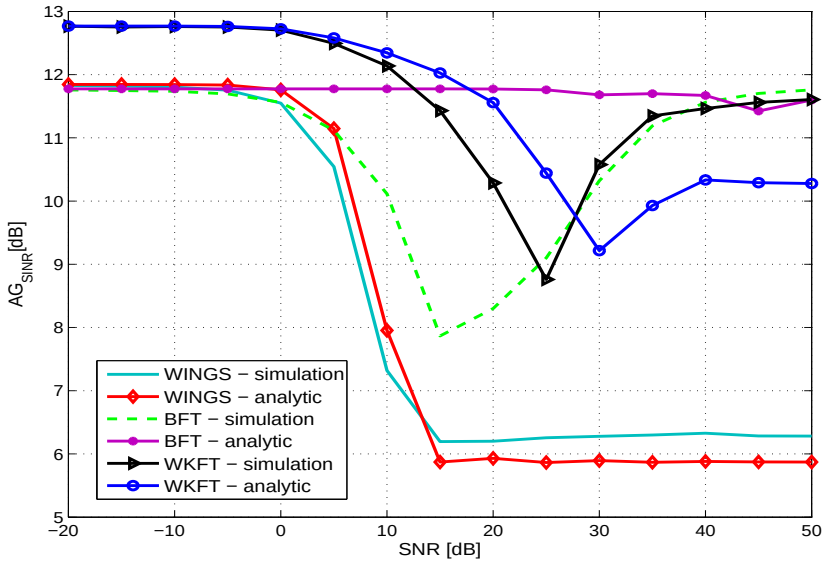

(a)

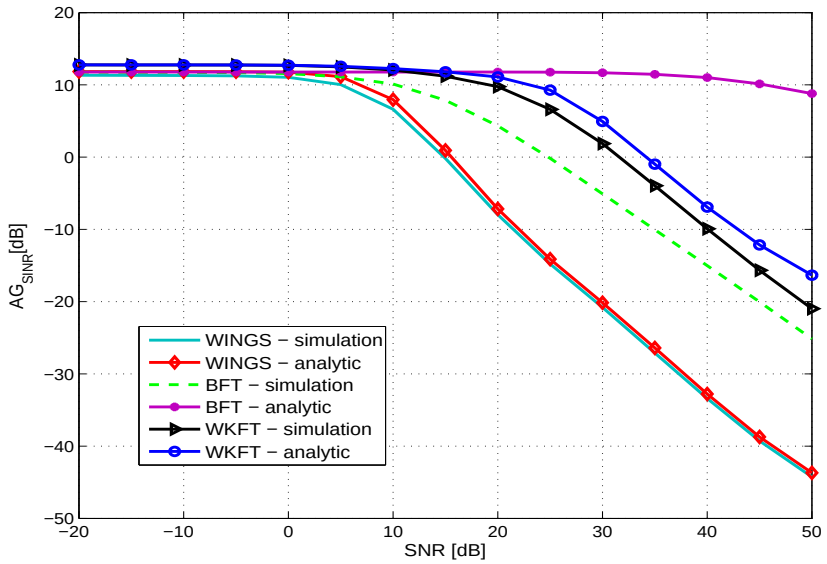

(b)

Figure 3.4: Array gain versus SNR for BFT, WINGS and WKFT for the case of one source and DOA uncertainty. (a) With Q-loading, (b)Without Q-loading

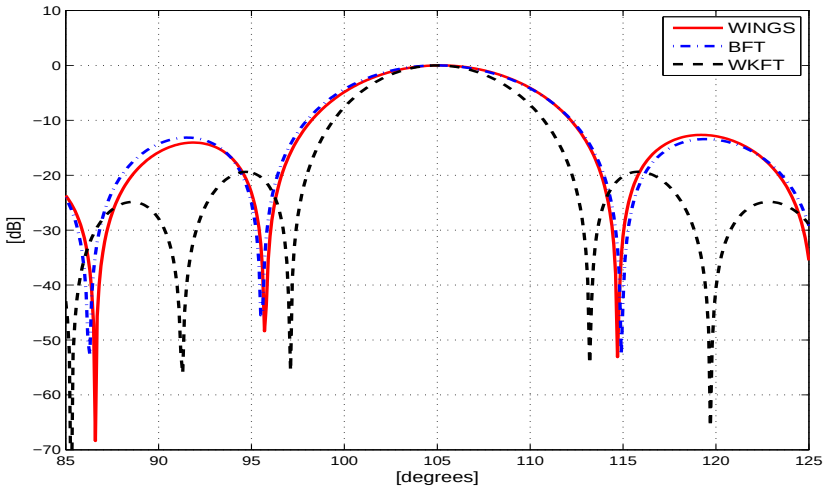

(a)

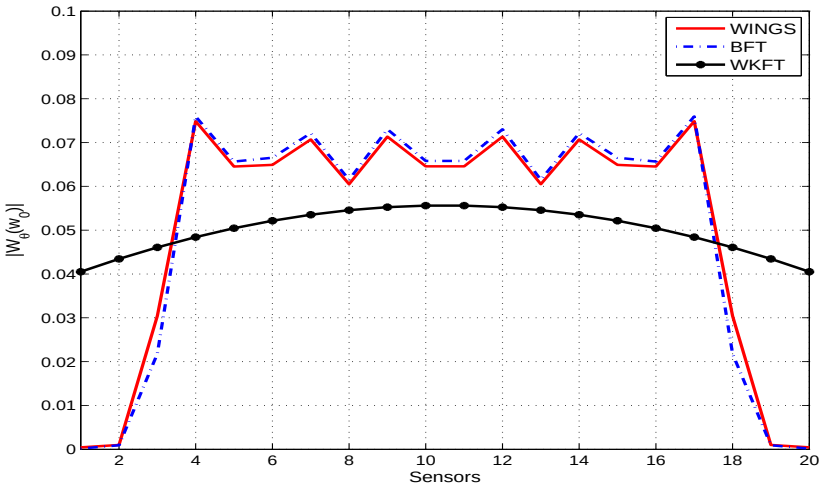

(b)

Figure 3.5: (a) Beampattern versus angle for the various methods for the one source case and $SNR = -10$dB , (b)Absolute value of the MVDR coefficients vector versus sensors for the various methods for the one source case and $SNR = -10$dB

Chapter 4

Reducing the Sensitivity of the Focused Wideband MVDR Beamformer to the Transformation Accuracy

4.1 Introduction

In the previous chapter, we investigated the performance of the focused MVDR beamformer in the presence of DOA uncertainties. We evaluated the performance of the BFT method which was presented in chapter 2 and compared it to that of the panoramic focusing WINGS method and of the WKFT method which require preliminary DOAs estimates. The results indicated a high sensitivity of the focused

MVDR to focusing errors in high SNR values for the various focusing methods. The AG degradation is especially large for the WINGS method which has relatively large focusing errors.

In this Chapter, we investigate this sensitivity and show analytically that it is caused due to focusing errors in the desired source direction. We will concentrate on a single source case whose DOA is assumed to be known perfectly.

In order to reduce the sensitivity of the coherent MVDR to focusing errors, we propose and study two robust methods for coherent focused wideband MVDR beamforming. The first method is based on modifying the MVDR beamformer by implementing a robust General-Rank (GR) beamforming scheme and the second is based on modifying the focusing transformation so that the focusing error is reduced in the direction of the desired source. A numerical study demonstrates a significant performance improvement of the proposed robust schemes when applied. Throughout this chapter, we examine the WINGS [22] focusing method in order to demonstrate the performance degradation due to focusing error and the improvement achieved by the robust proposed methods. We study WINGS method because it is a panoramic focusing method and hence, is not influenced by DOA uncertainties, so we can analyze the sensitivity to focusing error more simply.

This chapter is organized as follows: in Section 4.2, we conduct a numerical and simulative study for the single source case using the WINGS focusing method. In Section 4.3, we derive an analytic approximation to the degradation of the AG as a function of the focusing errors and the SNR. We show analytically that this

degradation occurs due to focusing error in the desired source direction. We also show that the AG deteriorates as the reciprocal of the squared SNR. In order to overcome the sensitivity to focusing errors we propose in Section 4.4 two robust schemes for wideband focused beamforming. In Section 4.5, we conduct a performance analysis demonstrating the efficacy of the proposed methods. Finally, we summarize this chapter in Section 4.6.

4.2 Sensitivity to Focusing Error

The results of Section 3.4 show a considerable sensitivity of the wideband focused MVDR to focusing errors for high SNR values. To investigate this sensitivity, we will analyze the single source case whose DOA is assumed to be known perfectly. We consider the WINGS method as a test case since it is a panoramic focusing method which is not influenced by the DOAs uncertainties.

Let us examine the AG for the single source case in the presence of additive white noise and perfect knowledge of its DOA. The simulation parameters are identical to those of Section 2.5. Fig. 4.1 shows the asymptotic and the simulative AG versus SNR for the coherent focused WINGS MVDR beamformer. Also shown is the performance when a loading term was added to the covariance matrix before inversion. This operation limits the norm of the beamformer coefficients vector yielding a robust beamformer (for more details see Chapter 3). We can see that the loading term improves the performance especially in high SNR values. Yet, in both cases we can see a significant decrease in the AG as the SNR increases. The performance of WINGS followed by the unloaded MVDR is severely degraded in

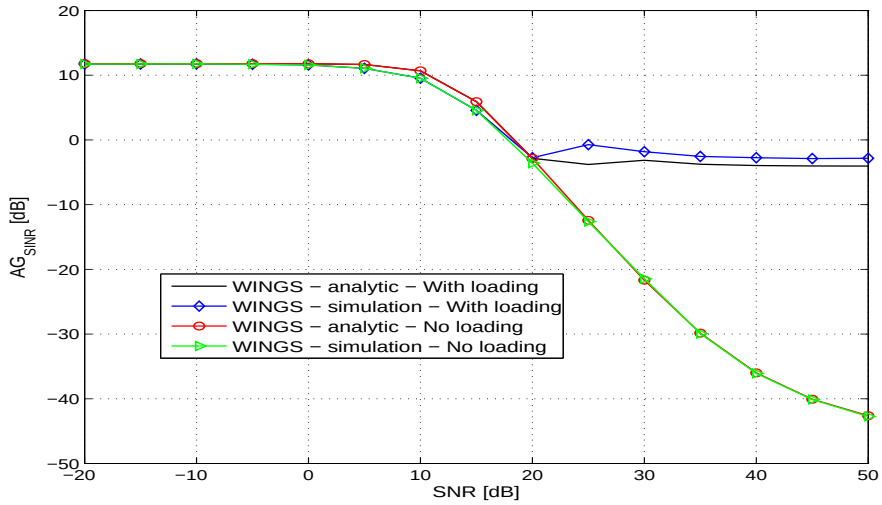

Figure 4.1: AG versus SNR, for the case of a single source and perfect knowledge of its DOA. With and without loading.

high SNR values. The fact that the degradation also occurs in the single source case and also in the analytic curve implies that the performance is very sensitive to a focusing error in the desired source direction, and less sensitive to focusing errors in the interferences DOAs. In the following section, we investigate this degradation and show analytically that it occurs due to the focusing error in the desired source direction.

4.3 Sensitivity to Focusing Error for the case of a Single Frequency

In this section, we derive an analytic approximate expression for the AG in the single frequency case. We attempt to provide some insight into the performance

degradation by analytically studying the case of a single frequency focusing transformation from w_j to w_0. From the results of the previous section we saw that without loading, the degradation is very severe, thus, the following analysis treats the unloaded MVDR case. We statistically model the focusing errors and show analytically how the AG decreases as the SNR increases in the presence of focusing error. The following analysis is based on modelling the focusing errors as small random independent perturbations of the amplitudes and the phases of the elements of the focused steering vector. A similar model has been used in [40], in order to analyze the sensitivity of the MVDR to amplitude and phase errors of the sensors. We now may write the mth element of the focused steering vector from frequency w_j to w_0 as

$$[\mathbf{T}(w_j)\mathbf{a}_\theta(w_0)]_m = a_{\theta,m}(w_0)(1+\Delta a_m(w_j)+j\Delta\phi_m(w_j)) \triangleq a_{\theta,m}(w_0)(1+\Delta g_m(w_j)), \tag{4.1}$$

where $a_{\theta,m}(w_0) = \exp^{j(\psi_m(w_0))}$ is the ideal focused steering vector, and $\Delta g_m(w_j)$ represents a zero-mean complex gain error of the mth sensor. We assume that the random gain errors are independent from sensor to sensor and have the same variance given by

$$\sigma_g^2(w_j) \triangleq E\left[|\Delta g_m(w_j)|^2\right], \quad m = 1,..,N \tag{4.2}$$

The focused data vector at frequency w_j is given by

$$\mathbf{x}^f(w_j) = s(w_j)\mathbf{a}_\theta^f(w_0,w_j) + \mathbf{T}(w_j)\mathbf{n}(w_j). \tag{4.3}$$

where $s(w_j)$ in the desired signal component at frequency w_j. $\mathbf{n}(w_j)$ is the additive noise at frequency w_j which is assumed to be a zero-mean white Gaussian process with variance σ_n^2. For the sake of simplicity we assume $\mathbf{T}(w_j)$ to be unitary, then the focused covariance matrix $\mathbf{R}_x^f(w_j, w_0)$ can be expressed as

$$\mathbf{R}_x^f(w_j, w_0) = \sigma_s^2(w_j)\mathbf{a}_\theta^f(w_0, w_j)(\mathbf{a}_\theta^f(w_0, w_j))^H + \sigma_n^2(w_j)\mathbf{I} \tag{4.4}$$

where $\sigma_s^2(w_j)$ in the power of the desired signal at w_j. The weight vector of the focused MVDR beamformer is given by

$$\mathbf{w}_\theta^f = \frac{(\mathbf{R}_x^f(w_j, w_0))^{-1}\mathbf{a}_\theta(w_0)}{\mathbf{a}_\theta^H(w_0)(\mathbf{R}_x^f(w_j, w_0))^{-1}\mathbf{a}_\theta(w_0)} \tag{4.5}$$

It can be shown that the output AG of the focused MVDR beamformer is (See appendix A.3)

$$\mathrm{AG} = \frac{N + \sigma_g^2}{(1 + (N-1)\sigma_g^2\xi)^2 + (N-1)(N + \sigma_g^2)\sigma_g^2\xi^2} \xrightarrow{\xi \gg 1} \alpha\frac{1}{\xi^2} \tag{4.6}$$

where ξ in the input SNR. Equation (4.6) indicates that the output AG is inversely proportional to ξ^2 for $\xi \gg 1$. In order to examine the quality and validity of the statistical approximation, Fig.4.2(a) compares the analytic (3.17) and approximated (4.6) AG received by BFT and WINGS methods for the case of a single frequency $f = 1710$Hz which has been focused to a lower frequency $f_0 = 1500$Hz. The case of a single frequency $f = 1240$Hz which has been focused to a higher frequency $f_0 = 1500$Hz is depicted at Fig.4.3(a). Figs. 4.2(b),4.2(c) and 4.3(b),4.3(c) plot

the corresponding focusing errors versus sensor index. We can see from Fig.4.2(a) that for focusing a high frequency onto a lower one, we get a relatively good fit of the analytic (3.17) and the approximated (4.6) AG, especially in the WINGS method. The AG begin decreasing at a rate of $1/\xi^2$ from $\xi \approx 20dB$ for the BFT and from $\xi \approx -10dB$ for the WINGS. The relatively small and roughly uniform errors in Figs 4.2(b) and 4.2(c) and the good fit of (3.17) and (4.6) justify the statistical approximation in this case. In Fig.4.3(a) we see a significant difference between the analytic and approximated AG when focusing a low frequency onto a higher one. This is because of the highly non uniform distribution of the focusing error across the array at both BFT and WINGS as illustrated in figs 4.3(b) and 4.3(c). In this case the statistical model assumptions are not valid and the approximated AG (4.6) may not be used. However we note that also in this case we observe a rate decay of $1/\xi^2$ in the WINGS as predicted by (4.6). So (4.6) provides some insight for the degradation of the AG in high SNR values in the presence of a focusing error, especially when focusing from high frequency to a lower one.

In the next section we propose two methods to reduce the sensitivity to focusing errors in high SNR values.

4.4 Robust MVDR Focused Beamformers for Coherent Wideband Array Processing

In this section we propose and examine two methods designed to combat the problem of sensitivity of the focused MVDR at high SNR values.

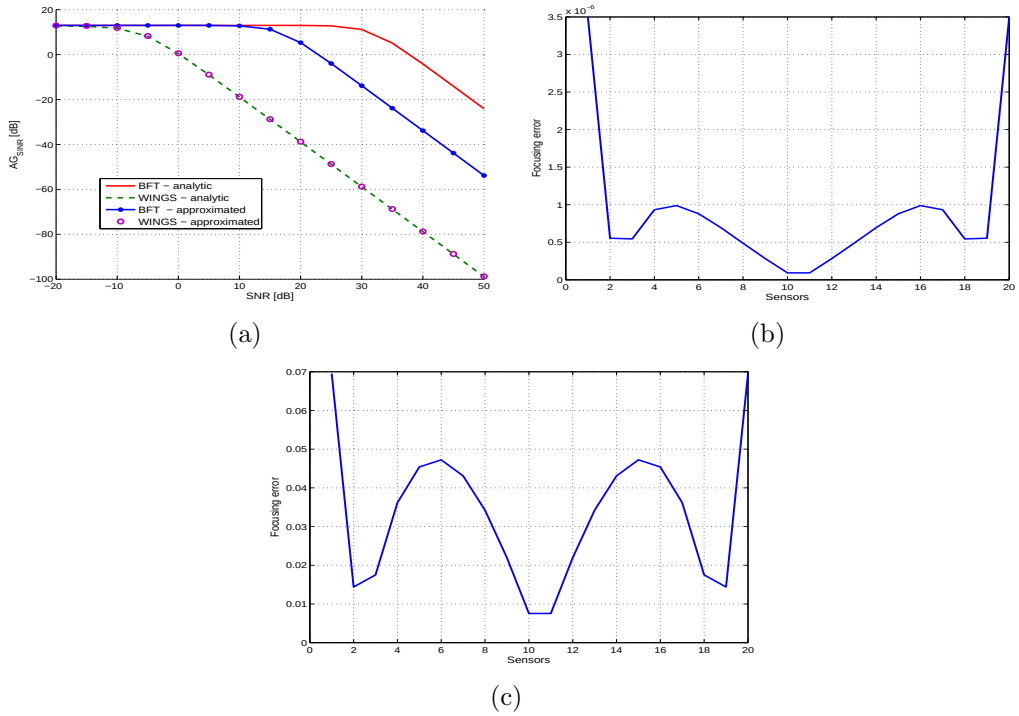

(a) (b)

(c)

Figure 4.2: (a) The analytic AG (3.17) for BFT (solid) and WINGS (dashed), and the approximated AG (4.6) for BFT (stars) and WINGS (circles) for the case of a single frequency $f_j = 1710$Hz transformed to the focusing frequency $f_0 = 1500$Hz. (b) Transformation error vs. sensor index - BFT. (c) Transformation error vs. sensor index - WINGS.

4.4.1 General-Rank Focused MVDR (GR-MVDR)

Let us examine more closely the structure of the signal component in the focused covariance matrix $\mathbf{R}_x^f$ (3.8). Inserting $\mathbf{R}_x(w_j) = \sigma_s^2(w_j)\mathbf{a}_{\theta_d}(w_j)\mathbf{a}_{\theta_d}^H(w_j) + \mathbf{R}_n(w_j)$ into (3.8) we get

$$\mathbf{R}_x^f = \mathbf{R}_s^f + \sum_{j=1}^{J} \mathbf{T}(w_j)\mathbf{R}_n(w_j)\mathbf{T}^H(w_j) \tag{4.7}$$

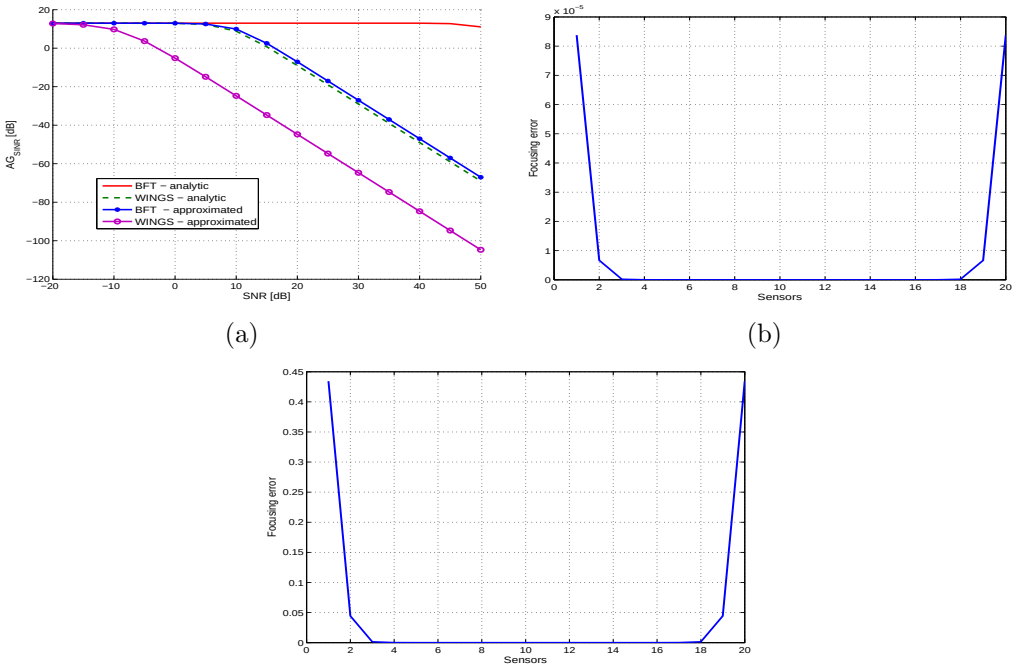

Figure 4.3: (a) The analytic AG (3.17) for BFT (solid), and for WINGS (dashed), the approximated AG (4.6) for BFT (stars) and for WINGS (circles) for case of a single frequency $f_j = 1240$Hz transformed to the focusing frequency of $f_0 = 1500$Hz . (b) Transformation error vs. sensor index - BFT. (c) Transformation error vs. sensor index - WINGS.

where $\mathbf{R}_s^f$ is the signal component of the focused covariance matrix

$$\mathbf{R}_s^f = \sum_{j=1}^{\mathbf{J}} \sigma_s^2(w_j)\mathbf{T}(w_j)\mathbf{a}_{\theta_d}(w_j)\mathbf{a}_{\theta_d}^H(w_j)\mathbf{T}^H(w_j). \tag{4.8}$$

From the above structure we see that the rank of the signal component covariance is larger than one. Therefore, we should use the general rank MVDR beamformer e.g. [41]. For the case where the source spectrum $\sigma_s^2(w_j)$ is known, we may find the Minimum Variance solution for the weight vector by maintaining a distortionless

array response to the signal covariance

$$\min_{\mathbf{w}} \mathbf{w}^H(w_0)\mathbf{R}_x^f\mathbf{w}(w_0) \;\; \textit{subject to } \mathbf{w}^H(w_0)\mathbf{R}_s^f\mathbf{w}(w_0) = \mathbf{1}. \tag{4.9}$$

Following [41], the solution of (4.9) is given by

$$\mathbf{w}_{\mathrm{GR-MVDR}}^f = \mathcal{P}\left\{(\mathbf{R}_x^f)^{-1}\mathbf{R}_s^f\right\}, \tag{4.10}$$

where $\mathcal{P}\{\cdot\}$ denotes the *principal eigenvector* of a matrix.

Robust GR-MVDR for the focused wideband MVDR

In [41] a robust version handling the uncertainties in the knowledge of $\mathbf{R}_x^f$ is also derived, based on the concept of the narrowband diagonal loading. We now extend the robust narrowband version of [41] to the focused wideband case. We are interested in limiting the white noise gain of the beamformer. In case of the focused beamformer, the output noise power is given by

$$\sigma_{n_{out}}^2 = \sigma_n^2(\mathbf{w}_\theta^f)^H \left(\frac{1}{J}\sum_{l=1}^{J}\mathbf{T}(w_l)\mathbf{T}^H(w_l)\right)\mathbf{w}_\theta^f, \tag{4.11}$$

where we assume that the noise spectrum is frequency independent, i.e. $\sigma_n^2(w) = \sigma_n^2, \forall w$. Thus, limiting the white noise gain yields the following additional quadratic constraint

$$(\mathbf{w}_\theta^f)^H\mathbf{Q}\mathbf{w}_\theta^{\mathbf{f}} \leq T_0, \tag{4.12}$$

where $\mathbf{Q} \triangleq \frac{1}{J}\sum_{l=1}^{J}\mathbf{T}(w_l)\mathbf{T}^H(w_l)$ and T_0 is a design parameter. Solving (4.9) with the additional constraint (4.12), by using the lagrange multipliers method, we get

$$(\mathbf{R}_x^f + \beta\mathbf{Q})^{-1}\mathbf{R}_s\mathbf{w}_\theta^f = \frac{1}{\lambda}\mathbf{w}_\theta^f. \tag{4.13}$$

The solution to (4.13) is given by the robust Q-loaded form of the GR-MVDR

$$\mathbf{w}_{\mathrm{GR-MVDR-QL}}^f = \mathcal{P}\left\{(\mathbf{R}_x^f + \beta\mathbf{Q})^{-1}\mathbf{R}_s^f\right\}, \tag{4.14}$$

where β is the loading factor. Note that the GR focused MVDR requires a-priori knowledge of the spectral shape of the source $\sigma_s^2(w_j)$. In practice the spectral density should be estimated. Following [41] we use a robust version combating a small signal spectrum mismatch

$$\mathbf{w}_{\mathrm{ROBUST-GR-MVDR}}^f = \mathcal{P}\left\{(\mathbf{R}_x^f + \beta\mathbf{Q})^{-1}(\mathbf{R}_s^f - \varepsilon\mathbf{I})\right\}, \tag{4.15}$$

where ε is the norm of the error in $\mathbf{R}_s^f$. Since the robust version is required for high SNR values, reasonably accurate PSD estimation of the source spectrum should be possible.

4.4.2 Enhanced Focusing (EF)

This method attempts to reduce the focusing error directly, and will be presented for WINGS focusing. WINGS has a relatively large focusing error due to the panoramic focusing requirement. Adding an additional error component in the

desired source direction to the LS minimization term (1.12) of the WINGS enables us to reduce the error in the source direction. In this case, the minimization term of the WINGS (1.8) becomes:

$$\varepsilon_j^2 = \frac{1}{N} \left\| [\widetilde{\mathbf{G}}(w_0) - \mathbf{T}(w_j)\widetilde{\mathbf{G}}(w_j)] \right\|_F^2 , \tag{4.16}$$

where

$$\widetilde{\mathbf{G}}(w) = [\mathbf{a}_{\theta_d}(w) \ , \ \mathbf{G}(w)] \tag{4.17}$$

and θ_d is the desired source direction. This solution achieves better performance as shown in the next section. Yet, it requires an accurate estimation of the desired source direction which is a drawback. In order to increase the robustness to DOA uncertainties, we add 4 auxiliary directions at $-2, -1, 1, 2$ degrees relative to the assumed desired source direction. In this case, (4.17) becomes

$$\widetilde{\mathbf{G}}(w) = [\mathbf{a}_{\theta_d-2}(w), \mathbf{a}_{\theta_d-1}(w), \mathbf{a}_{\theta_d}(w), ..., \mathbf{a}_{\theta_d+2}(w), \ \mathbf{G}(w)] \, . \tag{4.18}$$

Fig. 4.4 illustrates the benefit of adding the auxiliary directions. We can see that WINGS-EF with the auxiliary directions as in (4.18) is robust to direction errors of approximately 2 degrees.

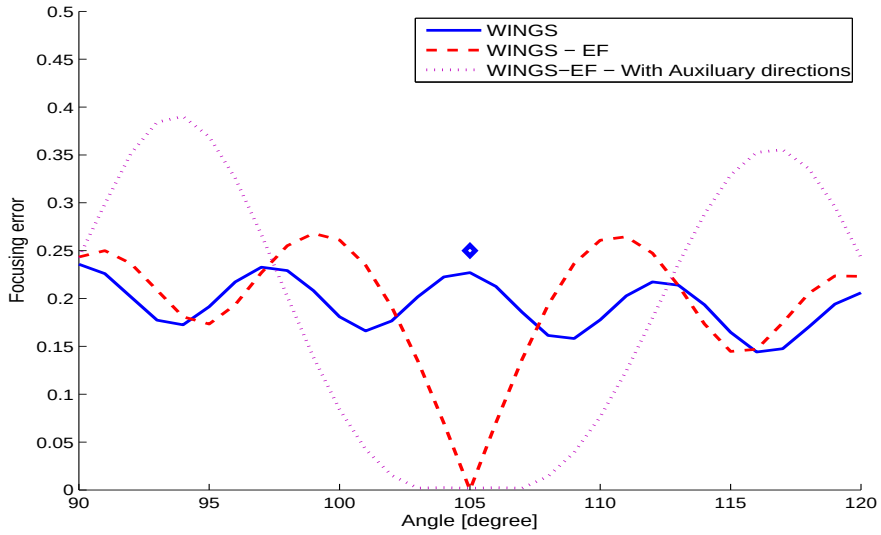

Figure 4.4: Focusing error versus angle for the various robust methods. Also presented the non-robust WINGS for comparison. The diamond marks the true source direction.

4.5 Performance Analysis of the Robust Focused MVDR

In this section, the performance of the proposed robust focused MVDR schemes, is numerically studied for the single source case. The simulation parameters are identical to those in Section 2.5. The signal spectrum which is required for the GR-MVDR is assumed to be flat in accordance with the simulation. There is an error at the desired source direction of 1.5 degrees.

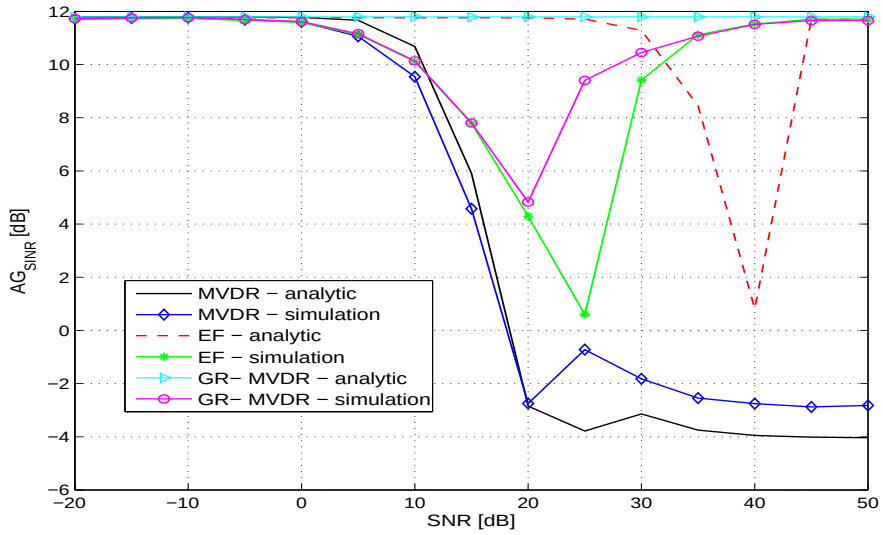

Figure 4.5: AG versus SNR of the various solutions for robust focused WINGS Q-loaded MVDR. Single source case with DOA error of 1.5 degrees.

4.5.1 Sensitivity to Source DOA

Fig.4.5 shows the analytic and simulative AG versus SNR of the focused WINGS-MVDR robust and non robust methods with a loading term. One can see that both robust schemes improve the performance of the focused WINGS MVDR, bringing the AG closer towards the ideal values. Both methods exhibit robustness to the DOA error.

4.5.2 Sensitivity to Source Spectrum

In this section we examine the sensitivity of the focused GR-MVDR to errors in the spectral shape of the source. Note that we assume a flat signal spectrum in accordance with the above example in which, white Gaussian sources were

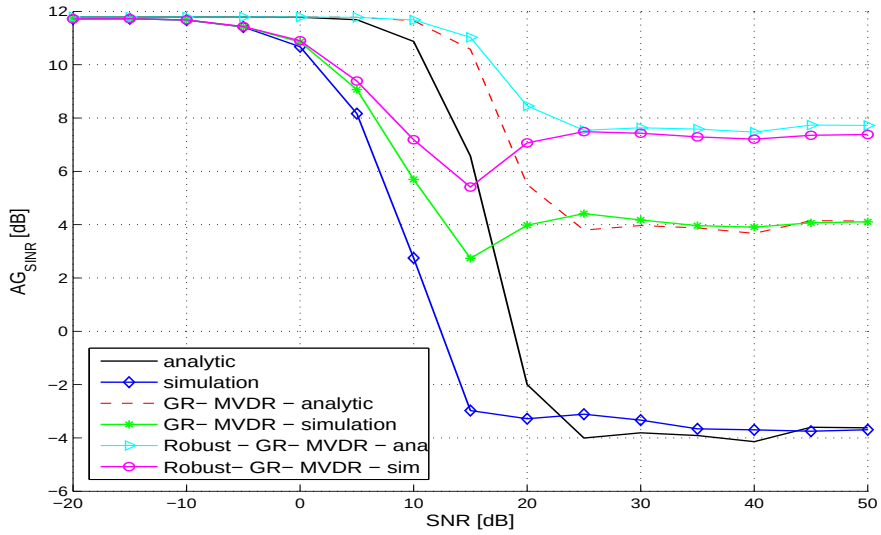

Figure 4.6: Array gain of the GR-MVDR solution for AR source spectrum with a known DOA. A maximal deviation of 3.5dB.

simulated. Figs. 4.6 and 4.7 demonstrate the performance of the focused GR-MVDR method when the source is shaped by an Auto-Regressive filter of a single pole whose spectrum is plotted at Fig. 4.8. In Figs. 4.6 and 4.7 we examine, respectively, 3.5dB and 1dB maximal spectral deviation between the actual and the assumed spectrum. From these examples we see that the robust extension of the focused GR-MVDR method (4.15) can handle a spectral deviation smaller than 1dB. In practice, for a larger deviation, spectrum estimation of the desired source should be used.

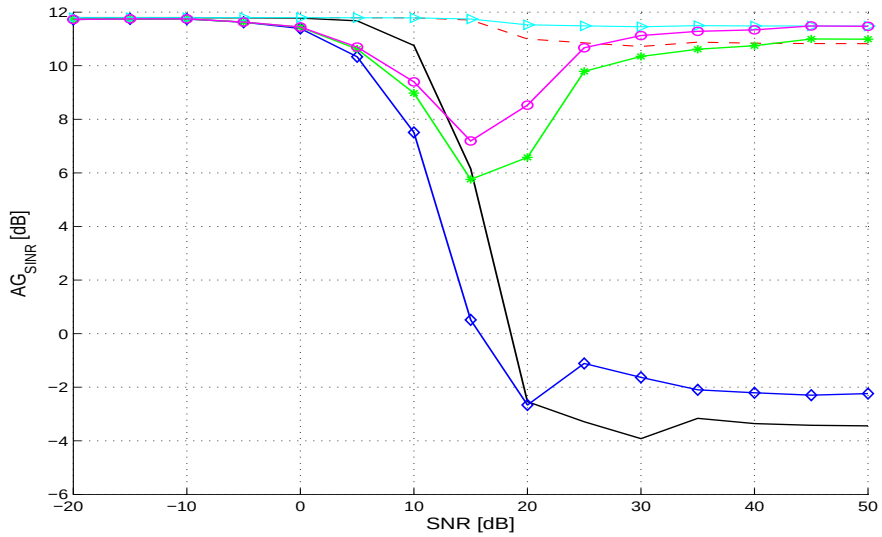

Figure 4.7: Array gain of the GR-MVDR solution for AR source spectrum with a known DOA. A maximal deviation of 1dB. The legend is like in fig. 4.6.

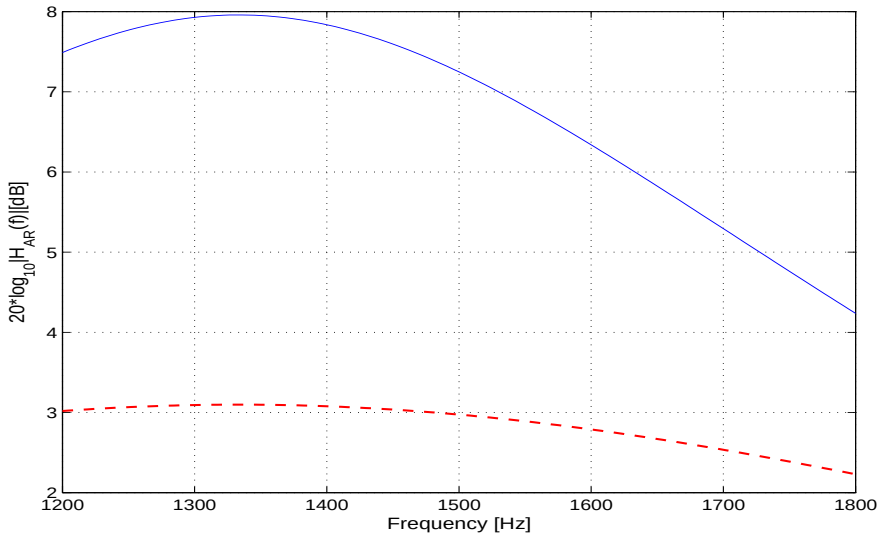

Figure 4.8: Spectrum of the Auto-Regressive signal. 1dB maximal deviation (dashed) and 3.5dB maximal deviation (solid).

4.6 Summary

We investigated the sensitivity of the focused MVDR beamformer to focusing errors in high SNR values and show analytically that the output AG of the focused MVDR is inversely proportional to the squared SNR. In order to reduce this sensitivity, we proposed and investigated two robust methods for wideband focused beamforming. The proposed methods aim at reducing the sensitivity of the beamformer's performance to focusing error, especially at high SNR scenarios. This sensitivity is more significant in interpolation based focusing methods which do not require preliminary estimates of the DOAs but have higher focusing errors. This independence of the focusing procedure on the preliminary DOAs estimates is a desirable property, therefore, designing robust MVDR beamformers for interpolation based focusing schemes is of importance. The first robust method is based on modifying the MVDR beamformer using the General-Rank (GR) approach, and the second is based on modifying the focusing scheme itself. We examine the proposed methods by applying them to the WINGS focusing transformation. The results indicate that both EF and GR-MVDR focusing methods can improve the performance of the WINGS significantly, especially at high SNR values. The GR-MVDR requires a spectral source estimation and the EF method requires an estimation of the desired signal DOA. However, the GR-MVDR method is computationally advantageous over the EF method, since spectral estimation is considerably less complex than data dependent calculation of the focusing transformations.

Chapter 5

Conclusion

5.1 Summary

In this work, we have proposed and investigated a Bayesian approach for focusing transformation design, which takes into account the statistical uncertainties in the DOAs during the focusing process. The focusing transformation block serves as a preprocessor stage of the wideband adaptive beamformer aiming at transforming the steering vectors of the array onto a fixed steering vector matched to a specific frequency, thus, allowing the use of a narrowband adaptive beamforming algorithm. The proposed Bayesian focusing approach is a compromise between the directional focusing approach which requires preliminary DOA estimates, and the panoramic focusing approach which is based on spatial interpolation and does not require any DOA estimates. A close form solution to the BFT is derived using a weighted extension of the WINGS focusing approach. The solution to the Bayesian focusing problem yields an optimal MMSE focusing transformation and

consequently an improved focused beamformer with better AG.

The proposed BFT approach requires the conditional PDFs of the DOAs to be available. In practice, they are not known perfectly and should be estimated from the received data. In order to estimate them, we proposed a time progressing algorithm which consists of two stages, the first performs DF on the focused vector and the second stage is the focused beamformer algorithm.

Adaptive beamformers such as the MVDR have a high sensitivity to focusing errors, and to other modelling errors such as gain and phase calibration errors, source direction errors, and covariance matrix estimation errors. This sensitivity can be reduced in the narrowband case by employing the diagonal loading procedure. In this work we derived the Q-loaded wideband focused SMI-MVDR beamformer, which is a generalization of the diagonal loading scheme suitable to the focused wideband beamformer.

The Q-loaded focused MVDR beamformer employs a generalized *transformation-dependent* loading of the sample covariance matrix, thus taking into account the focusing process in the robust version. This yields superior robustness to the focused beamformer, compared to that of the popular diagonal loading method.

We evaluated the performance of the proposed BFT method and other focusing methods by conducting simulations and comparing their results to the analytic expression of the AG which was derived earlier. The results illustrate the superiority of the proposed BFT method for the multi-source case in DOA uncertainties conditions compared to that of the WINGS and WKFT focusing methods. This

is attributed to the low focusing error of the BFT across the entire bandwidth, which yields more accurate focused data. The significant improvement in the performance and robustness of the focused Q-loaded MVDR beamformer with respect to that of the un-loaded MVDR was also demonstrated.

The simulation results demonstrate a consistent degradation in the performance of WINGS and WKFT methods as the SNR increased. We investigate this degradation and show analytically that it occurs due to the focusing error in the desired source direction. There is a rate decay of $1/\xi^2$ where ξ is the input SNR.

In order to reduce this sensitivity, we proposed and studied two robust methods for coherent focused wideband MVDR beamforming. The proposed methods aim at reducing the sensitivity of the beamformer's performance to focusing error, especially at high SNR scenarios. This sensitivity is more significant in interpolation based focusing methods which do not require preliminary estimates of the DOAs but have higher focusing errors. The first robust method is based on modifying the MVDR beamformer applying the General-Rank (GR) approach, and the second is based on modifying the focusing scheme itself. We examined the proposed methods by applying them to the WINGS focusing transformation.

5.2 Future Research

The methods we have proposed in this work open several interesting directions for future study:

1. In this work we assumed that the sources propagate at a free medium. This

assumption is lenient since the impulse response of the channel is not taken into account. One of the effects of a typical channel is the multipath effect which causes reflected versions of the signal to be received by the array. This leads to a singular source covariance matrix due to perfect coherence between the signal and its reflections, and as a consequence, to the signal cancellation problem, which is a serious drawback in adaptive beamformers. In [28] a steered wideband adaptive beamformer optimized by a maximum likelihood criterion is presented and discussed in the light of a very general reverberation model. Yet, the proposed channel model is fairly simplistic. Note that the focusing procedure decorrelates the covariance matrix of the received vector [13], thus removing the singularity due to the correlated signals. In light of the above, an analytic and simulative study of the BFT in more realistic reverberant multipath environment is of considerable interest.

2. The BFT focusing procedure requires apriori knowledge of the PDFs of the DOAs or an estimated version of them. We modelled them as gaussian random variables where we estimated their mean using a DF algorithm and assumed their variance to be a fixed value equal to a quarter of the 3dB beamwidth. A possible improvement would be to take the CRB of the estimations produced by the DF algorithm to be the variance of the gaussian PDFs. This allows us to take into account other parameters which supposed to influence the PDF, such as SNR. A different approach would be to model the DOAs using a Markov chain. The motivation is to model not only the DOAs themselves but also the connection between DOAs estimates produced

at different times.

3. The BFT was developed using a weighted extension of the WINGS method [22]. It is designed to provide a focusing method which is robust to DOAs uncertainties. In practice, there are other array calibration errors which should be taken into account. We take care of them by employing the Q-loaded MVDR beamformer. In [22] two robust extensions to the WINGS method are presented aiming at increasing the robustness to the noise gain of the transformation which can be caused also because of array calibration errors. Employing this robust extensions also to the BFT will yields a focusing method which is robust to both DOA uncertainties and array calibration errors.

4. In Section 2.5 it was demonstrated that WINGS introduces high errors at frequencies below the focusing frequency. This is expected since WINGS is an interpolation based focusing method, in which focusing is equivalent to spatial interpolation [18] of the array. Interpolating from a low frequency to a higher one, is equivalent to extrapolating the array beyond its physical length, thus, yielding high focusing errors. One can reduce the WINGS transformation error by focusing to the lowest frequency of the bandwidth. However, this will reduce the effective aperture of the focused array, thus reducing the spatial resolution of the array. In the literature there are several papers dealing with the issue of choosing the optimal focusing frequency (e.g. [38, 39]). It is expected that optimization of the focusing frequency for the BFT as well as for other focusing transformations will also can improve

its performance.

5. BFT is a non-unitary focusing method. In the literature the benefits of a unitary focusing transformation is demonstrated [9]. In [24] a unitary focusing transformation which employing a weighting function is derived. Combining both the Bayesian approach and the unitary approach of [24] is expected to yield a considerably more robust focusing method.

6. In Chapter 3 we demonstrate the performance degradation in low SNR values in interpolation based approaches (see Fig.3.5(b)). This degradation is significant especially in the single source case where the adaptive beamformer is reduced to the conventional beamformer, since the array beamwidth is widened. It is of interest to further investigate this degradation and to find techniques to reduce it when using interpolation based methods.

7. In Chapter 4 we proposed and investigated two robust methods aiming to handle the sensitivity in high SNR values due to focusing error in the desired source direction. This study can be extended to other focusing methods such as the unitary focusing transformation proposed in [24].

8. In this work, the issue of computational complexity of the BFT was not considered and compared to other focusing methods. It is desirable to evaluate this complexity and to search for techniques to reduce it.

Appendix A

A.1 Derivation of (3.6)

Using the method of *Lagrange multipliers* to solve (3.5a)-(3.5c), the function to be minimize is

$$F = (\mathbf{w}_\theta^f)^H \mathbf{R}_x^f \mathbf{w}_\theta^f + \beta \left[(\mathbf{w}_\theta^f)^H \mathbf{Q} \mathbf{w}_\theta^{\mathbf{f}} - T_0 \right] + \lambda \left[\mathbf{a}_\theta^H(w_0) \mathbf{w}_\theta^f - 1 \right] + \left[(\mathbf{w}_\theta^f)^H \mathbf{a}_\theta(w_0) - 1 \right] \lambda^H. \tag{A.1}$$

Taking the gradient with respect to $\mathbf{w}_\theta^f$ and setting the result to zero gives

$$(\mathbf{w}_\theta^f)^H \mathbf{R}_x^f + \beta (\mathbf{w}_\theta^f)^H \mathbf{Q} + \lambda \mathbf{a}_\theta^H(w_0) = 0, \tag{A.2}$$

or

$$(\mathbf{w}_\theta^f)^H = -\lambda \mathbf{a}_\theta^H(w_0) \left[\beta \mathbf{Q} + \mathbf{R}_x^f \right]^{-1}. \tag{A.3}$$

Solving for λ by substituting (A.3) into (3.5b) yields (3.6). Note that the above derivation is an extension of the well known diagonal loading solution which is

used for the narrowband case.

A.2 Proof that $\mathbf{w}^H\mathbf{Q}\mathbf{w}$ is a monotonically decreasing function of β

Let us define

$$\tilde{\mathbf{a}}_\theta(w_0) = \mathbf{Q}^{-\frac{1}{2}}\mathbf{a}_\theta(w_0) \tag{A.4}$$
$$\bar{\mathbf{R}}_x^f = \mathbf{Q}^{-\frac{1}{2}}\mathbf{R}_x^f\mathbf{Q}^{-\frac{1}{2}},$$

substituting (A.4) into (3.6), we get

$$\mathbf{w}_\theta^f = \frac{\mathbf{Q}^{-\frac{1}{2}}\left(\bar{\mathbf{R}}_x^f + \beta\mathbf{I}\right)^{-1}\tilde{\mathbf{a}}_\theta(w_0)}{\tilde{\mathbf{a}}_\theta^H(w_0)\left(\bar{\mathbf{R}}_x^f + \beta\mathbf{I}\right)^{-1}\tilde{\mathbf{a}}_\theta(w_0)}. \tag{A.5}$$

Now, calculating $(\mathbf{w}_\theta^f)^H\mathbf{Q}\mathbf{w}_\theta^\mathbf{f}$ we get

$$(\mathbf{w}_\theta^f)^H\mathbf{Q}\mathbf{w}_\theta^\mathbf{f} = \frac{\left\|\left(\bar{\mathbf{R}}_x^f + \beta\mathbf{I}\right)^{-1}\tilde{\mathbf{a}}_\theta(w_0)\right\|^2}{\left(\tilde{\mathbf{a}}_\theta^H(w_0)\left(\bar{\mathbf{R}}_x^f + \beta\mathbf{I}\right)^{-1}\tilde{\mathbf{a}}_\theta(w_0)\right)^2} = h(\beta). \tag{A.6}$$

$h(\beta)$ has the form of the diagonal loading constraint for which there is a well-known proof that it is a monotonically decreasing function of β, see e.g [1] p.589.

A.3 Derivation of (4.6)

Defining:

$$\mathbf{G} = \begin{bmatrix} 1+\Delta g_1(w_j) & 0 & \cdot & \cdot & 0 \\ 0 & 1+\Delta g_2(w_j) & \cdot & \cdot & 0 \\ \cdot & \cdot & \cdot & \cdot & \cdot \\ \cdot & \cdot & \cdot & \cdot & \cdot \\ 0 & 0 & \cdot & \cdot & 1+\Delta g_N(w_j) \end{bmatrix} \tag{A.7}$$

The covariance matrix for the case of a single source with a single frequency w_j is

$$\mathbf{R} = \sigma_d^2(w_j)\tilde{\mathbf{a}}_\theta(w_j)\tilde{\mathbf{a}}_\theta^H(w_j) + \sigma_n^2(w_j)\mathbf{I}, \tag{A.8}$$

where $\tilde{\mathbf{a}}_\theta(w_j) = \mathbf{G}\mathbf{a}_\theta(w_j)$. Using Woodbury's Identity [32], the inverse of (A.8)

$$\mathbf{R}^{-1} = \sigma_n^{-2}\frac{(1+\xi\tilde{\mathbf{a}}_\theta^H(w_j)\tilde{\mathbf{a}}_\theta(w_j))\mathbf{I} - \xi\tilde{\mathbf{a}}_\theta(w_j)\tilde{\mathbf{a}}_\theta^H(w_j)}{1+\xi\tilde{\mathbf{a}}_\theta^H(w_j)\tilde{\mathbf{a}}_\theta(w_j)}, \tag{A.9}$$

where $\xi \triangleq \frac{\sigma_d^2(w_j)}{\sigma_n^2(w_j)}$. The SINR in the beamformer output is

$$SINR = \frac{\mathbf{w}^H(w_j)\tilde{\mathbf{a}}_\theta(w_j)\tilde{\mathbf{a}}_\theta^H(w_j)\mathbf{w}(w_j)}{\mathbf{w}^H(w_j)\mathbf{w}(w_j)}, \tag{A.10}$$

where $\mathbf{w}(w_j)$ is the MVDR beamformer coefficient vector.

It can be shown that $E\{\tilde{\mathbf{a}}_\theta^H(w_j)\tilde{\mathbf{a}}_\theta(w_j)\} \overset{N>>1}{\rightarrow} N(1+\sigma_g^2(w_j))$ where

$$\sigma_g^2(w_j) \triangleq E\left[|\Delta g_m(w_j)|^2\right], \quad m = 1,..,N. \tag{A.11}$$

Substituting the last result and the MVDR coefficient vector expression into (A.10) yields (4.6).

Bibliography

[1] H. L. Van-trees, *Detection, estimation and modulation theory, Part IV - optimum array processing.* New York: Wiley Interscience, 2002.

[2] T. S. Rappaport, *Smart Antennas.* New York: IEEE Press, 1998.

[3] A. J. Paulraj and C. B. Papadias, "Space-time processing for wireless communications," *IEEE Signal Processing Mag.*, vol. 14, pp. 49 – 78, Nov. 1997.

[4] T. Do-Hong and P. Russer, "Signal processing for wideband smart antenna array applications," *IEEE Microwave Mag.*, vol. 5, pp. 57 – 67, Mar. 2004.

[5] S. Ohmori, Y. Yamao, and N. Nakajima, "The future generations of mobile communications based on broadband access technologies," *IEEE Commun. Mag.*, vol. 38, pp. 134 – 142, Dec. 2000.

[6] S. Haykin, *Adaptive Filters Theory.* Englewood Cliffs, New Jersey: Prentice-Hall, 4nd ed., 2001.

[7] H. Wang and M. Kaveh, "Coherent signal-subspace processing for the detection and estimation of angles of multiple wide band sources," *IEEE Trans.*

on Acoustics, Speech and Signal Processing, vol. ASSP-33, pp. 823–831, Aug. 1985.

[8] H. Wang and M. Kaveh, "On the performance of signal-subspace processing - part ii: Coherent wide-band systems," *IEEE Trans. on Acoustics, Speech and Signal Processing*, vol. ASSP-34, pp. 1201–1209, Oct. 1986.

[9] H. Hung and M. Kaveh, "Focusing matrices for coherent signal subspace processing," *IEEE Trans. on Acoustics, Speech and Signal Processing*, vol. 36, pp. 1272–1281, Aug. 1988.

[10] J. X. Zau and H. Wang, "Adaptive beamforming for correlated signal and interference: a frequency domain smoothing approach," *IEEE Trans. on Acoustics, Speech and Signal Processing*, vol. 38, pp. 193–195, Jan. 1990.

[11] J. F. Wang and M. Kaveh, "Coherent signal-subspace transformation beamformer," *IEE Proceedings, Pt. F*, vol. 137, pp. 267–275, Aug. 1990.

[12] Y. H. Chen and F. P. Yu, "Broadband adaptive beamforming based on coherent signal subspace using spatial interpolation preprocessing," *Radar and Signal Processing, IEE Proceedings F*, vol. 138, pp. 489–494, Oct. 1991.

[13] S. Simanapalli and M. Kaveh, "Broad band focusing for partially adaptive beamforming," *IEEE Trans. on Aerospace and Electronic Systems*, vol. 30, pp. 68–80, Jan. 1994.

[14] A. Zeira and B. Friedlander, "Interpolated array minimum variance beamforming for correlated interference rejection," *Proceedings IEEE Int. Conf.*

Acoustics, Speech and Signal Processing (ICASSP), vol. 6, pp. 3165–3168, May. 1996.

[15] M. A. Doron and A. J. Weiss, "On focusing matrices for wide-band array processing," *IEEE Trans. Signal Processing*, vol. 40, pp. 1295–1302, Jun. 1992.

[16] H. S. Hung and C. Y. Mao, "Robust coherent signal-subspace processing for directions-of-arrival estimation of wideband sources," *IEE Proceedings of Radar, Sonar and Nevigation*, vol. 141, pp. 256–262, Oct. 1994.

[17] M. A. Doron, E. Doron, and A. J. Weiss, "Coherent wide-band processing for arbitrary array geometry," *IEEE Trans. Signal Processing*, vol. 41, pp. 414–417, Jan. 1993.

[18] J. Krolik and D. Swingler, "Focused wide-band array processing by spatial resampling," *IEEE Trans. on Acoustics and Speech Signal Processing*, vol. 38, pp. 356–360, Feb. 1990.

[19] T. S. Lee, "Efficient wideband source localization using beamforming invariance technique," *IEEE Trans. Signal Processing*, vol. 42, pp. 1376–1387, Jun. 1994.

[20] H. Kashavarz, "Weighted signal subspace direction finding of ultra wideband sources," *IEEE Trans. Signal Processing*, vol. 42, pp. 2549–2559, Oct. 2005.

[21] B. Friedlander and A. J. Weiss, "Direction finding for wide-band signals using an interpolated array," *IEEE Trans. Signal Processing*, vol. 41, pp. 1618–1634, April 1993.

[22] M. A. Doron and A. Nevet, "Robust wavefield interpolation for adaptive wideband beamforming," *Signal Processing*, vol. 80, pp. 1579–1594, Jan. 2008.

[23] M. A. Doron and E. Doron, "Wavefield modeling and array processing; part i - spatial sampling," *IEEE Trans. Signal Processing*, vol. 42, pp. 2549–2559, Oct. 1994.

[24] F. Sellone, "Robust auto-focusing wideband doa estimation," *Signal Processing*, vol. 86, pp. 17–37, Jan. 2006.

[25] X. Feng, J. Huang, Q. Zhang, and H. Wang, "A novel doa estimation method and its focusing matrices for multiple wide-band sources," *IEEE Int. Conf. Neural Network and Signal Processing*, vol. 42, pp. 1306–1309, Dec. 2003.

[26] T. D. Hond and P. Russer, "Wideband direction-of-arrival estimation in the presence of array imperfection and mutual coupling," *IEEE Microwave and Wireless Componenets Letters*, vol. 13, pp. 314–316, Aug. 2003.

[27] T. D. Hond and P. Russer, "An analysis of wideband direction-of-arrival estimation for closely-spaced sources in the presence of array model errors," *IEEE Microwave and Wireless Componenets Letters*, vol. 13, pp. 314–316, Aug. 2003.

[28] E. D. D. Claudio, "Robust ml wideband beamforming in reverbrant fields," *IEEE Trans. Signal Processing*, vol. 51, pp. 338–349, Feb. 2003.

[29] E. D. D. Claudio, "Optimal quiescent vectors for wideband ml beamforming in multipath fields," *Signal Processing*, vol. 85, pp. 107–120, Feb. 2005.

[30] J. Capon, "High resolution frequency-wavenumber spectrum analysis," *Proc. IEEE*, vol. 57, pp. 1408–1418, Aug. 1969.

[31] H. Cox, "Resolving power and sensitivity to mismatch of optimum array processors," *J. Acoust. Soc. Amer.*, vol. 54, pp. 771–785, Jul. 1973.

[32] G. H. Golub and C. F. Van-Loan, *Matrix computations.* The Johans Hopkins University Press, 2nd ed., 1989.

[33] B. D. Carlson, "Covariance matrix estimation errors and diagonal loading in adaptive arrays," *IEEE Trans. Aerosp. Electron. Syst.*, vol. 24, pp. 397–401, Jul. 1988.

[34] H. Cox, R. M. Zeskind, and M. M. Owen, "Robust adaptive beamforming," *IEEE Trans. Acoust., Speech, Signal Processing*, vol. 35, pp. 1365–1376, Oct. 1987.

[35] C. C. Lee and J. H. Lee, "Robust adaptive array beamforming under steering vectors errors," *IEEE Trans. Antennas Propagat.*, vol. 45, pp. 168–175, Jan. 1997.

[36] R. O. Schmidt, "Multiple emitter location and signal parameter estimation," *in Proc. RADC Spectral Estimation Workshop, Griffiths AFB, Rome, NY*, 1979.

[37] S. Simanpalli and M. Kaveh, "Broadband focusing for partially adaptive beamforming," *IEEE Trans. on Aerosp.Electron.Syst.*, vol. 30, pp. 68–80, Jan. 1994.

[38] S. Valaee and P. Kabel, "The optimal focusing subspace for coherent signal subspace processing," *IEEE Trans. on Signal Processing*, vol. 44, pp. 752–756, Mar. 1996.

[39] D. Swingler, P. Kabel, and J. Huang, "Source location bias in the coherently focused high - resolution broad band beamformer," *IEEE Trans. Acoust, Speech, Signal Processing*, vol. 37, pp. 143–145, Jan. 1989.

[40] W. S. Youn and C. K. Un, "Robust adaptive beamformering based on the eigenstructure method," *IEEE Trans. on Signal Processing*, vol. 42, pp. 1543–1547, Jun. 1994.

[41] S. Shahbazpanahi, A. B. Gershman, Z. Luo, and K. M. Wong, "Robust adaptive beamforming for general-rank signal models," *IEEE Trans. Signal Processing*, vol. 9, pp. 2257–2269, Sep. 2003.

טרנספורמציות מיקוד בייסיאניות לעיצוב אלומה קוהרנטי אדפטיבי רחב סרט

חיבור על המחקר

לשם מילוי חלקי של הדרישות לקבלת התואר
מגיסטר למדעים בהנדסת חשמל

יעקב בוכריס

הוגש לסנט הטכניון - מכון טכנולוגי לישראל
תמוז תש״ע חיפה יוני 2010

המחקר נעשה בהנחיית פרופסור ישראל כהן מהפקולטה להנדסת חשמל וד״ר מרים דורון מרפאל. ברצוני להודות לשניהם על הדרכתם המסורה, על העידוד לשלמות ועל העצות המועילות לאורך כל שלבי המחקר.

ברצוני גם להודות לרפאל – הרשות לפיתוח אמצעי לחימה בע״מ
על התמיכה הכספית והמקצועית במחקר זה

אחרונים חביבים, תודה מיוחדת לאישתי האהובה, אורית, ולילדי, תאיר ואליה-אבידן . לא הייתי מצליח להשלים את העבודה הזו ללא תמיכתם ואהבתם.

תקציר

טכניקות עיצוב אלומה מסתגל משמשות במגוון אפליקציות ברחבי העולם כגון: תקשורת אלחוטית, רדאר, סונאר, אקוסטיקה ועוד. טכניקות אלו משמשות להשגת שבח עיבוד מרחבי עבור האות הרצוי, במקביל לדיכוי אותות חוסמים המהווים הפרעות לאות הרצוי, ואשר מגיעים מכיוון השונה מזה של האות הרצוי. עיבוד מרחבי באמצעות שיטות עיצוב אלומה מסתגלות קיים כבר משנות השישים עבור המקרה הצר סרט, אולם בשני העשורים האחרונים גבר באופן משמעותי הצורך באלגוריתמי עיצוב אלומה רחבי סרט עם התפתחות מערכות דור שלישי ורביעי של תקשורת אלחוטית כמו גם מערכות תקשורת רחבות סרט. במערכות אלו נעשה שימוש באותות רחבי סרט ובעיבוד מרחבי לצורך השגת קצבי תקשורת גבוהים יותר.

ניתן לחלק את השיטות לעיצוב אלומה רחב סרט לשתי קטגוריות עיקריות. הקטגוריה הראשונה הינה קטגורית העיבוד הלא קוהרנטי אשר כוללת הן שיטות בתחום הזמן והן שיטות בתחום התדר. שיטות לא קוהרנטיות בתחום הזמן עושות שימוש במשוונים מסתגלים מרחביים, ואילו שיטות לא קוהרנטיות בתחום התדר מממשות אלגוריתם עיצוב אלומה צר סרט עבור כל תדר ותדר בנפרד. החסרונות העיקריים של השיטות הלא קוהרנטיות הינם סיבוכיות חישוב גבוהה עקב מספר יחסית גדול של מקדמים שנדרש לשערך ולעדכן באופן מסתגל, התכנסות איטית לפתרון האופטימאלי ובעיות של פגיעה באות הרצוי בסביבות קורלטיביות, כגון סביבות רברברציות ורב נתיב.

הקטגוריה השנייה של שיטות לעיצוב אלומה מסתגל רחב סרט הינה קטגורית העיבוד הקוהרנטי. שיטות השייכות לקטגוריה זו עושות שימוש בהתמרות מיקוד (Focusing Transformations) שהן התמרות ליניאריות, אשר ממקדות את תתי המרחב תלויי התדר של האות לתת מרחב יחיד המתואם לתדר המיקוד. כתוצאה מפעולת המיקוד, האות הממוקד היו אות עם תכולה ספקטראלית רחבת סרט אבל בעל כיווניות צרת סרט ולכן ניתן לבצע עליו עיצוב אלומה צר סרט, למשל, באמצעות אלגוריתם ה – Minimum Variance Distortionless Response (MVDR). היתרונות העיקריים של השיטות הקוהרנטיות על פני הלא-קוהרנטיות הינם סיבוכיות חישוב יחסית נמוכה, התכנסות מהירה יותר לפתרון האופטימאלי והתמודדות טובה יותר עם בעיית ביטול אות רצוי בסביבות קורלטיביות .

בספרות קיימות שתי גישות עיקריות על מנת לתכנן את התמרות המיקוד עבור העיבוד הקוהרנטי. הגישה הראשונה הינה גישה כיוונית אשר בה נדרש לדעת את כיווני ההגעה של המקורות, ופעולת המיקוד מבוצעת בכיוונים אלו. הגישה השנייה הינה גישה פנוראמית המבוססת על אינטרפולציה מרחבית ואשר בה פעולת המיקוד מבוצעת עבור כל הכיוונים האפשריים. הגישה הכיוונית רגישה לאי וודאות בידיעת כיווני ההגעה האמיתיים של המקורות אולם בעלת שגיאת מיקוד נמוכה יחסית. לעומתה, הגישה הפנוראמית הינה בעלת שגיאת מיקוד גבוהה יחסית אולם לא רגישה לאי וודאות בכיוונים.

בעבודה זו פיתחנו ובחנו גישה בייסיאנית לתכנון התמרות המיקוד לעיצוב אלומה קוהרנטי רחב סרט הנקראות - Bayesian Focusing Transformations (BFT). הגישה הבייסיאנית מכלילה את שתי הגישות הקודמות ומנצלת את היתרונות שלהן ולכן מאפשרת השגת חסינות גדולה יותר לשגיאות כיוון ביחד עם הקטנת שגיאות המיקוד. הגישה הבייסיאנית לוקחת בחשבון את הפילוגים ההיסתברותיים של כיווני ההגעה וממזערת את שגיאת המיקוד הריבועית הממוצעת של התמרת המיקוד על פני כל רוחב הסרט של האותות.

בנוסף, פיתחנו הרחבה רובסטית למעצב האלומה הקוהרנטי מבוסס MVDR אשר מטרתה הקטנת הרגישות של מעצב האלומה הממוקד לשגיאות הנגרמות כתוצאה מאי וודאות בכיווני ההגעה של המקורות, שגיאות הגבר ופאזה, שגיאות שערוך של מטריצת הקוואריאנס, ובפרט שגיאות המיקוד. הכללנו את פתרון ה – Diagonal Loading שפותח במקור על מנת להגביל את הרעש במוצא ה - MVDR צר הסרט והתאמנו אותו ל – MVDR רחב הסרט הממוקד. האלגוריתם שהתקבל נקרא Q-Loaded Focused MVDR.

ביצועי התמרות ה – BFT בשילוב עם ה - Q-Loaded Focused MVDR נבדקו והושוו לביצועי מספר התמרות מיקוד ידועות:

- התמרת WKFT(Wang and Kaveh Focusing Transformation) – הינה השיטה המקורית שהוצעה ע"י Wang ו – Kaveh הממקדת בכיוונים המשוערכים של המקורות.
- התמרת ה- RSS(Rotational Signal Subspace) – הינה שיטת מיקוד כיוונית יוניטרית שהוצעה ע"י Hung ו – Kaveh . היתרון בהתמרה יוניטרית הינו שאין פגיעה ב - SNR כתוצאה מפעולת המיקוד.

- התמרת ה - (Wavefield Interpolated Narrowband Subspace) WINGS – הינה שיטת מיקוד פנוראמית שהוצעה ע"י Doron ו - Nevet.

תוצאות סימולציית מונטה-קרלו וחישובים נומריים מדגימות שיפור משמעותי בהגבר המערך של ה - Focused Q-Loaded MVDR מבוסס BFT על פני יתר ההתמרות, בתרחישים של מספר מקורות ואי וודאות בכיווני ההגעה שלהם. השיפור בביצועים הינו כתוצאה משגיאת מיקוד נמוכה יותר של התמרת ה – BFT בהשוואה להתמרות האחרות שנבדקו. בהתמרות האחרות שנבדקו, שגיאת המיקוד הייתה גבוהה יחסית, הן כתוצאה מאי הוודאות בכיווני ההגעה המשפיעה מאד על השיטות הכיווניות, והן כתוצאה משגיאה גבוהה בשיטות הפנוראמיות עקב הניסיון למקד על פני תחום רחב של כיוונים. יתר על כן, התוצאות הראו שיפור משמעותי כאשר נעשה שימוש ב - Q-Loading.

תופעה מעניינת נוספת שהודגמה בסימולציות הינה ירידה בביצועי כל השיטות בערכי SNR גבוהים. אמנם ירידה זו הינה קטנה יותר כאשר נעשה שימוש ב – Q-loading אולם עדיין מהווה בעיה משמעותית בביצועים. חקרנו רגישות זו והראנו אנליטית כי היא נגרמת בעיקר כתוצאה משגיאות מיקוד בכיוון האות הרצוי, ושהביצועים יורדים באופן יחסי הפוך לריבוע ה - SNR. על מנת להקטין את הרגישות הזו, בחנו שתי שיטות לשיפור החסינות של עיצוב האלומה הקוהרנטי בערכי SNR גבוהים. השיטה הראשונה מבוססת על שינוי האילוץ של בעיית האופטימיזציה של ה – MVDR כך שתתחשב בשגיאת המיקוד (General-Rank MVDR), והשיטה השנייה מבוססת על הוספת אילוצים בתכנון התמרות המיקוד על מנת להקטין את השגיאה בכיוון האות הרצוי. תוצאות נומריות וסימולטיביות הראו שיפור ניכר בביצועי עיצוב האלומה הקוהרנטי גם עבור תחום ה – SNR הגבוה.